



OPEN ACCESS

EDITED BY

Martin Rücklin,
Naturalis Biodiversity Center,
Netherlands

REVIEWED BY

Michael Polcyn,
Southern Methodist University,
United States
Julia Brenda Desojo,
Consejo Nacional de Investigaciones
Científicas y Técnicas (CONICET),
Argentina

*CORRESPONDENCE

Megan Rose Woolley,
meganwoolley@live.co.za

SPECIALTY SECTION

This article was submitted
to Paleontology,
a section of the journal
Frontiers in Earth Science

RECEIVED 17 June 2022

ACCEPTED 07 November 2022

PUBLISHED 13 December 2022

CITATION

Woolley MR, Chinsamy A and
Caldwell MW (2022), Unraveling the
taxonomy of the South
African mosasaurids.
Front. Earth Sci. 10:971968.
doi: 10.3389/feart.2022.971968

COPYRIGHT

© 2022 Woolley, Chinsamy and
Caldwell. This is an open-access article
distributed under the terms of the
[Creative Commons Attribution License
\(CC BY\)](https://creativecommons.org/licenses/by/4.0/). The use, distribution or
reproduction in other forums is
permitted, provided the original
author(s) and the copyright owner(s) are
credited and that the original
publication in this journal is cited, in
accordance with accepted academic
practice. No use, distribution or
reproduction is permitted which does
not comply with these terms.

Unraveling the taxonomy of the South African mosasaurids

Megan Rose Woolley^{1*}, Anusuya Chinsamy¹ and
Michael Wayne Caldwell²

¹Department of Biological Sciences, Science Faculty, University of Cape Town, Cape Town, South Africa, ²Biological Sciences Department, Science Faculty, University of Alberta, Edmonton, AB, Canada

Until recently, only one mosasaur was identified in South Africa based on disarticulated skull bones including two dentary fragments and a frontal with articulated elements. These were discovered in 1901 in Pondoland, Eastern Cape and were initially described by Broom in 1912 when he assigned them to *Tylosaurus capensis*. Aside from this specimen, two other mosasaur remains are known but have remained undescribed and include an isolated muzzle unit and an isolated vertebra. The current study provides a morphological description and taxonomic interpretation of all the mosasaur remains discovered in South Africa. It is suggested that the specimen originally assigned to *Tylosaurus* is a mosaic of two taxa: A dentary fragment and frontoparietal show affinities with *Prognathodon*, while a second dentary fragment shows features similar to those of *Taniwhasaurus*. The muzzle unit presents *Prognathodon*-like features, and a more recently discovered incomplete vertebra is referred to as an indeterminate Plioplatecarpine. We therefore recognize at least three mosasaur taxa from the Late Cretaceous deposits of South Africa, which we tentatively refer to cf. *Prognathodon*, cf. *Taniwhasaurus*, and cf. Plioplatecarpinae. A shark tooth that was embedded in the matrix around the *Prognathodon* muzzle unit was identified as a *Squalicorax pristodontus* (Late Campanian to Late Maastrichtian). Strontium analysis of the mosasaur tooth enamel from the same muzzle unit of the cf. *Prognathodon* material was dated to Late Maastrichtian ($^{87}\text{Sr}/^{86}\text{Sr} = 0.707817$; age = 66.85Ma).

KEYWORDS

Prognathodon, *Tylosaurus*, mosasaur, strontium dating, *Taniwhasaurus*, *Squalicorax*, Pondoland, South Africa

Abbreviations: CDP, Council for Geosciences Pretoria, South Africa; CMN, Canadian Museum of Nature, Ottawa, Canada; SAM, South African Museum, Cape Town, South Africa; OCP, Office Chérifien des Phosphates; RBINS, Royal Belgian Institute for Natural Sciences, Brussels, Belgium; Royal Tyrrell Museum of Palaeontology, Drumheller, Canada; UCT, University of Cape Town, Cape Town, South Africa.

1 Introduction

Our knowledge of mosasaurs has been greatly expanded in the last century (Ellis, 2003), and it has recently been shown that mosasaur remains from South Africa (SA) are more extensive than previously realized (Jiménez-Huidobro, 2016; Chinsamy-Turan et al., 2018). The only descriptive and taxonomic work prior to this study, remains Broom's (1912) description of a frontal/parietal complex as *Tylosaurus capensis*. No interpretations or descriptions exist for the other specimens in SA collections. Given the paucity of mosasaurids from Southern Africa, providing new taxonomic assignments for the known specimens of SA mosasaurs helps to place these mosasaurs into the global temporal and geographic distribution of this group of marine squamates.

Mosasaurid remains from SA were first discovered in 1901 on the coast of Pondoland, Eastern Cape, and reported as such by Rogers and Schwarz (1902)—“a lower jaw resembling those belonging to the reptilian genus *Mosasaurus*”. This material was recovered from Cretaceous deposits on the south-west side of the Mzamba river, likely from a fossiliferous sequence within the Mzamba Formation (Liu and Greyling, 1996). These beds consisted of coarse shelly and sandy rocks with pebbles of dark slates and coarse grits or sandstones and were considered to be deposited in a storm-influenced marine environment (Susela, 2014). Although, the area and the mosasaur fossils discovered there have been considered to be Santonian in age (Rogers and Schwarz, 1902; Broom, 1912), the geology of the area is complex and so Liu and Greyling (1996) referred to the rocks in broad terms, as “Late Cretaceous”. Broom (1912) reported on the Pondoland material, but he only described a frontoparietal complex, and although he mentioned ‘some jaw fragments with teeth’, these jaw elements remained undescribed (Broom, 1912).

In 2016, an indeterminate mosasaurid partial vertebra was discovered from the Nibela Peninsula, St Lucia, KwaZulu-Natal, SA (Chinsamy-Turan et al., 2018). This area is estimated to be upper Campanian in age (Walaszczyk et al., 2009). There currently are no other known mosasaur discoveries in SA aside from those in Pondoland and St Lucia.

In this study, we describe the osteology and anatomy of the currently known SA mosasaur materials housed in two collections. Based on our anatomical descriptions we present tentative interpretations of generic level identity where possible, or higher clades when generic assignments are not possible. The materials described here are for the most part, poorly preserved, fragmentary specimens. The goal of this study is to characterize these specimens and place the known SA mosasaur specimens into a more global framework of mosasaurs in the Late Cretaceous.

2 Methods

2.1 Taxonomic methods

The published literature, as well as personal observations (MRW) of mosasaur specimens at the Royal Belgian Institute of Natural Sciences (RBINS) are used to compare the anatomical features of the SA mosasaur material (Table 1) with those of other mosasaurs for which the taxonomy is known.

Detailed photographs of the specimens were taken with a Canon Powershot sx 720 camera or a Huawei P30 mobile phone. Reconstructions and drawings were made using Microsoft 3D paint. Reconstructions were made by copying and horizontally flipping well-preserved areas of the specimens and then pasting them over the poorly preserved areas. This constructed image was then traced with a dotted line, before removing the constructed image and replacing it with an image of the actual specimen. Measurements were taken using digital callipers and a measuring tape (for the larger samples). Tables and calculations were done in Microsoft Excel.

A small amount of enamel from one of the fragmentary isolated teeth (IT-1) and from the shark tooth embedded in the matrix around the CGP/1/2265 was removed for comparative paleobiological purposes.

2.2 Strontium isotope analysis

Strontium isotope analysis was done in the multi-collector inductively coupled plasma mass spectrometry (MC-ICP-MS) facility, in the Department of Geological Sciences, University of Cape Town (UCT) using a laser ablation technique. An Australian Science Instruments RESOLUTION-SE laser ablation unit was coupled with a NuPlasma high-resolution multi-collector inductively coupled plasma mass spectrometry (HR-MC-ICP-MS) instrument. The operational parameters of the laser unit and mass spectrometer are outlined in Supplementary Table S1.

The ICP-MS instrument comprises 12 F cups fitted with 1011-ohm resistors, 3 ETP electron multiplier ion counters and one channeltron ion counter in a fixed-position collector

TABLE 1 Mosasaur material investigated in this study and their associated specimen numbers, element descriptions and locality.

Specimen	Skeletal element	Locality
SAM-PK-5265 (FC)	Frontoparietal complex	Pondoland
SAM-PK-5265 (PDF)	Posterior dentary fragment	Pondoland
SAM-PK-5265 (ADF)	Anterior dentary fragment	Pondoland
CGP/1/2265	Muzzle unit, isolated teeth and a shark tooth	Pondoland
NA	Isolated vertebra	St Lucia

array (Le Roux, 2010). The ion beam was manipulated using zoom optics in order to ensure alignment and coincidence of the ion beam of interest. The data from the MC-ICP-MS presented in this study were collected using 11 of the 12 F cup detectors (^{89}Y : H6 ^{88}Sr :H5, $^{87}\text{Sr}+$ ^{87}Rb :H4, $^{173}\text{Yb}++$:H3 $^{86}\text{Sr}+$ ^{86}Kr :H2, $^{171}\text{Yb}++$: H1 ^{85}Rb : Ax, $^{84}\text{Sr}+$ ^{84}Kr :L2, $^{166}\text{Er}++$:L3, $^{42}\text{Ca}^{40}\text{Ar}$:L4). The final $^{87}\text{Sr}/^{86}\text{Sr}$ data presented are therefore corrected for instrumental mass fractionation using the measured $^{86}\text{Sr}/^{88}\text{Sr}$ ratio and a stable value of 0.1194, and for isobaric interference at 87amu by ^{87}Rb using the measured ^{85}Rb signal and the natural Rb isotope ratio. Any potential interference due to doubly charged Yb and Er isotopes and Ca argides were monitored, and negligible corrections applied (Ramos et al., 2004).

Prior to the laser ablation, thin sections were made from the most fragmentary isolated tooth (IT-1) following methods outlined by Chinsamy and Raath (1992) at the Palaeobiology Lab, UCT. Laser ablation was performed directly on two thin sections to precisely pinpoint the tooth enamel as was done by Chinsamy et al. (2012). The thin sections were mounted on a holding tray and placed inside the laser ablation sample chamber. The enamel sample sites were chosen in regions of the enamel that were appropriate i.e., had no cracks and were wide enough for the laser to ablate the enamel only and not ablate part of the dentine or glass (see Figure 1). The sites were weakly ablated prior to doing the reading to remove potential surface

contamination (Copeland et al., 2008; Chinsamy et al., 2012). This initial cleaning sweep removed approximately the top 2–5 μm layer of the enamel with a 100 μm spot size. The data collection ablation analysis followed the pre-ablated path; however, the ablation involved a narrower laser beam of 80 μm with higher energy and a slower speed (like Copeland et al., 2008) and removed an approximately 20 μm deep layer from the enamel surface. A total of six isotopic measurements were collected from the enamel of IT-1, excluding one trial run (Figure 1).

2.3 Computed tomography scanning

A computed-tomography (CT) scan was performed on the muzzle unit at the UCT Private Hospital in Cape Town, SA using a Philips Brilliance 64 slice CT Scanner. The CT scans were analyzed using Mimics, a three-dimensional medical imaging software, which revealed additional details around the teeth, particularly the replacement teeth and other cranial elements that are not visible externally.

Micro-CT scans were done on the dentary fragment with replacement teeth (SAM-PK-5265) and the two isolated fragmentary teeth (IT-1 and IT-2 from CGP/1/2265) at X-Sight in Somerset West. The following parameters were used to scan all specimens: 190 kV (voltage); 550 μA (current) and 74 μm

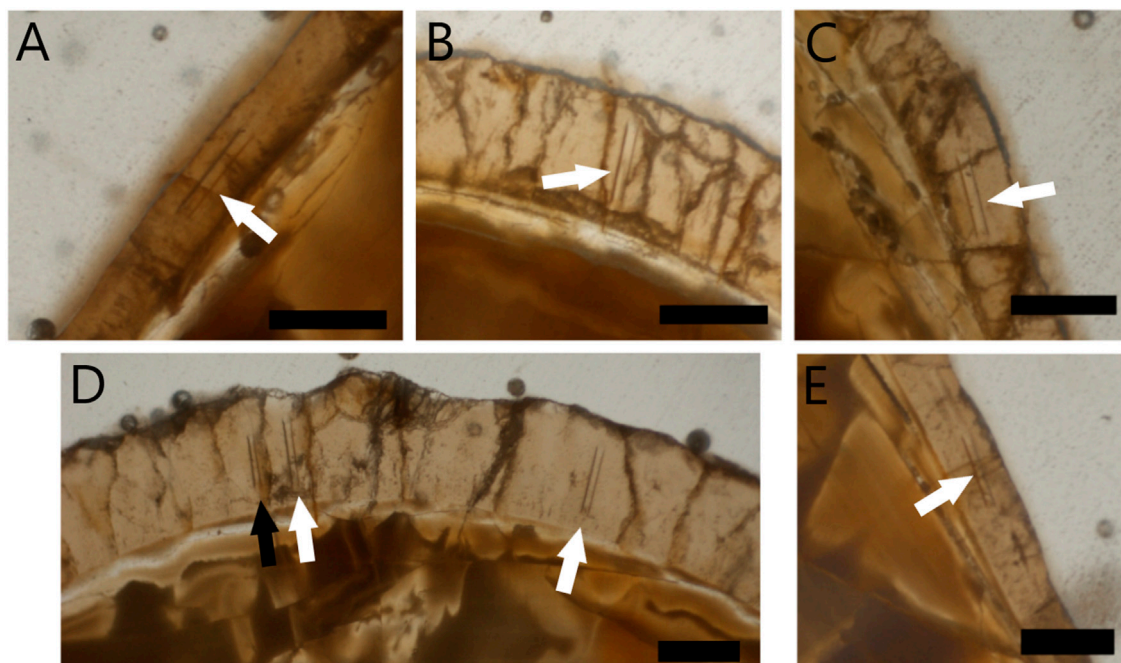


FIGURE 1

Laser ablated areas of enamel of two thin sections of isolated tooth 1 (IT-1) from cf. *Prognathodon* (CGP/1/2265). Two single thin sections represented (A–C) and (D,E). White arrows indicate regions where enamel was ablated for analysis and black arrow indicates initial trial ablation. Scale bars = 100 μm .

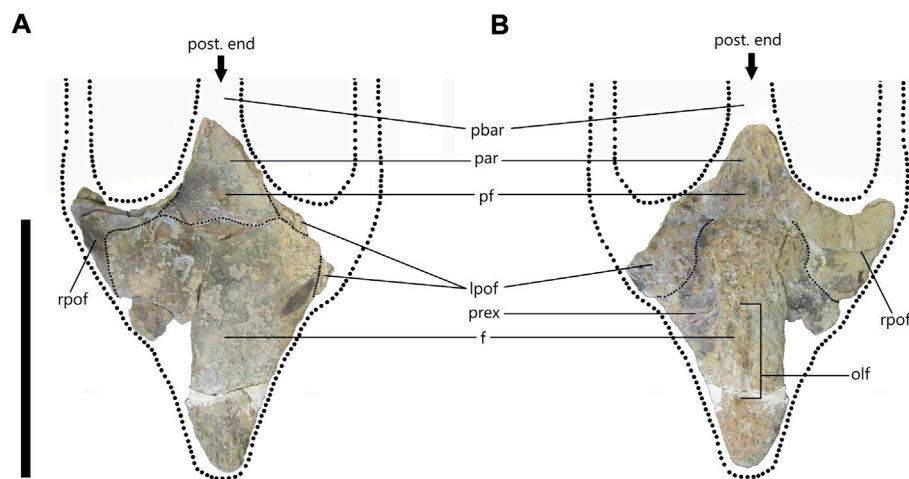


FIGURE 2

cf. *Prognathodon* (SAM-PK-5265) frontoparietal complex in dorsal (A) and ventral (B) views with dotted lines to reconstruct anterior portions of parietal bar and postorbitofrontal rami. (A) Fine, dotted lines indicate sinusoidal suture with 5 alae between frontal and postorbitofrontals and parietals. (B) Fine, dotted lines indicate sutures between frontal and postorbitofrontals. Abbreviations: frontal (f); left postorbitofrontal (lpof); olfactory tract (olf); parietal (par); parietal bar (pbar); pineal foramen (pf); prefrontal excavation (prex); right postorbitofrontal (rpof). Scale bar = 300 mm.

(resolution). MyVGL was used to analyze the scan data and save images. These images were edited using Microsoft Paint 3D.

3 Systematic Paleontology

SQUAMATA Oppel, 1811

MOSASAURIDAE Gervais, 1852

cf. *PROGNATHODON* Dollo, 1889 (Figures 2, 3)

Diagnosis—for an emended diagnosis, see Konishi et al. (2011).

Specimen and location—SAM-PK-5265 frontoparietal complex and posterior dentary fragment from the Cretaceous rocks southwest of the Mzamba River, Pondoland, Eastern Cape, South Africa.

Remarks—SAM-PK-5265 was originally described by Broom (1912) as *Tylosaurus capensis*. The material assigned by Broom (1912) to this holotype included one frontoparietal complex, an anterior dentary fragment with replacement teeth, and a posterior dentary fragment with no teeth. The frontoparietal complex includes an almost complete frontal bone and the articulated anterior portion of the parietal and portions of both postorbitofrontals. In revising Broom's (1912) interpretation of the material as the remains of a tylosaur, we present below a comparison of the material to both known tylosaur and prognathodontine genera and species.

Description—SAM-PK-5265 is comprised of four articulated cranial elements, namely an almost complete

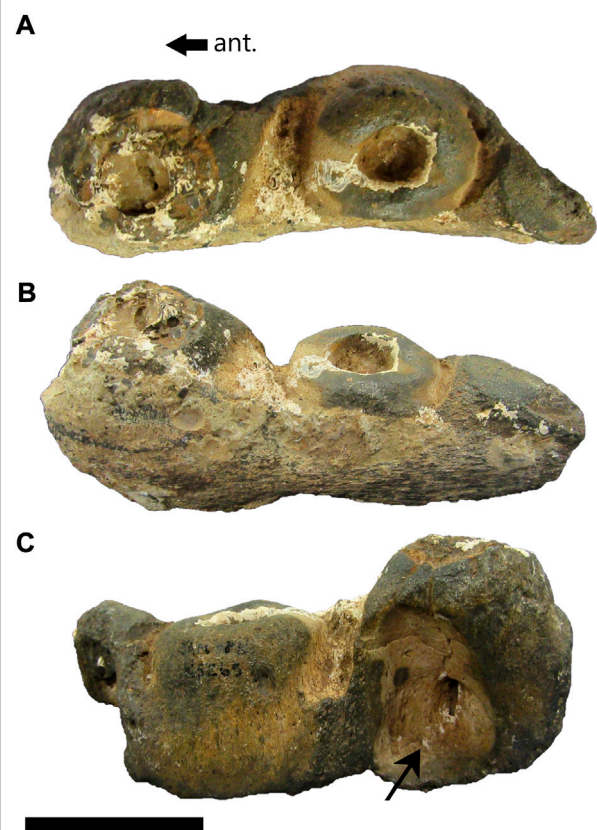


FIGURE 3

cf. *Prognathodon* (SAM-PK-5265) posterior dentary fragment in dorsal (A), lateral (B) and medial (C) views. Anterior (ant.) arrows pertain only to medial view. Black arrow in C points to large resorption pit visible on medial side. Scale bar = 50 mm.

frontal, and the anterior portion of the parietal and portions of both postorbitofrontals. Additional fossil preparation at the Iziko SA Museum in Cape Town revealed some new anatomical details, which are presented below.

3.1 Frontal

The frontal is mostly complete with some fragments missing near the middle-right side of the bone, as well as the anterior-left side, which has been filled-in with plaster. There are several cracks on the bone, particularly near the postorbitofrontal and parietal sutures. The anterior tip was reattached to the frontal with plaster (Figure 2A).

The frontal is broad posteriorly and narrows toward the anterior end. It is dorsoventrally compressed but is robust and thick in comparison to many of the other frontals observed at the RBINS, which indicated a large and heavy skull. It is approximately 43 mm thick in the center of the bone (near the posterior end of the olfactory tract) (Figure 2B) and approximately 10 mm thick where the prefrontal excavation is at the lateral edge of the bone. It also tends to decrease in thickness anteriorly with the anterior tip of the frontal being approximately 15 mm thick.

Overall, it is triangular with a length of 297 mm from the anterior tip to the apex of the median sutural flange. It has a maximum width of 235 mm from the posterolateral edges of the frontal, giving it a length to width ratio of 1.3:1. The anterior tip of the frontal is rounded and broad, which was noted by [Broom \(1912\)](#) who suggested that this mosasaur probably had separate nasal bones, which were not preserved, as in most specimens observed at RBINS. The lateral margins are almost straight, though reconstruction shows they bulge slightly towards the posterior end of the frontal (Figure 2A). Anteriorly, there is no evidence to suggest that the frontal contributed to the shape of the posterior margins of the external nares and there are no sutures visible that could indicate the internarial bar overlapped the anterior of the frontal. However, the anterior tip of the frontal is probably broken and therefore the shape could be an artifact of preservation.

The dorsal surface of the frontal is smooth and relatively flat. There is a slight indentation where the median sutural flange meets the parietal. This could indicate that the anterior portion of the parietal overlaps the posterior portion of the frontal. Alternatively, it could be an artifact of fossilization whereby the bones may have shifted slightly. The anterior half of the frontal bone has a low, blunt midline ridge about 175 mm long from the anterior tip of the frontal that extends posteriorly to form a flat surface. This is like the midline ridge visible on the frontals of two *Tylosaurus bernardi* specimens at RBINS (R020 and R023).

On the ventral surface of the frontal, the excavation or fossa for the left prefrontal is visible (Figure 2B). The right

postorbitofrontal is relatively complete compared to the left and is attached to the ventral side of the frontal. The olfactory lobe tract is a shallow excavation that is visible on the anterior half of the ventral surface and sits in line with the pineal foramen. The olfactory lobe tract terminates anteriorly before the anterior tip of the frontal and terminates posteriorly in line with the anteroventral corners of the postorbitofrontals.

There are five posterior sutural alae (crests) that form a sinusoidal suture with the postorbitofrontals and parietal (Figure 2A). These alae are all bluntly rounded and roughly the same width. The median ala forms a crest directly beneath the pineal foramen, which is unusual. Most mosasaur frontoparietal sutures observed at RBINS or seen figured, show one of four sutural forms: 1) a tight embayment around the pineal foramen; 2) pass through the pineal foramen; 3) are positioned beneath the pineal foramen with a gentle 'trough' that does not envelope the pineal foramen; 4) form a simple, straight suture beneath the pineal foramen.

3.2 Parietal

The parietal is incomplete with roughly half of the table broken off diagonally (Figure 2). Dorsally the parietal is smooth, but the surface preservation on the ventral side is not as good (Figure 2B). Only the anterior portions of the parietal are present. Neither the suspensorial rami nor parietal alae are preserved. Both the left and right postorbitofrontal processes of the parietal are preserved. The right side is more complete, but the cracks in this region make it impossible to see the sutures between the parietal and postorbitofrontals. However, by reconstructing the line that follows the edges of the lateral parietal bar it is possible to estimate the position of the sutures between parietal and postorbitofrontals (Figure 2A).

Although the parietal is dorsoventrally compressed, it is also thick and robust like the frontal. Just posterior to the pineal foramen, the parietal table has a dorsoventral thickness of 43 mm and is thicker still on the lateral edges due to the presence of lateral ridges. The pineal foramen is positioned 20.97 mm posterior to the frontoparietal suture and is infilled. Dorsally, the pineal foramen is almost circular in shape with a length of 13.17 mm and a width of 14.12 mm. Ventrally it is more oblong with a length of 26.36 mm and a width of 14.12 mm.

The right postorbitofrontal processes of the parietal and the right postorbitofrontal form the anterior boundary of the right supratemporal fenestra. The anterior margin of the supratemporal fenestra of SAM-PK-5265 is relatively rounded and resembles the type of *Prognathodon solvayi* (R033) ([Lingham-Soliar and Nolf, 1990](#)). Additionally, the parietal bar of *P. solvayi* is broad, as it is in SAM-PK-5265; however, the position of the pineal foramen and the shape of the frontoparietal sutures are inconsistent with those features in SAM-PK-5265. The immature *Tylosaurus proriger* specimen (CNM 8162),

originally figured by [Stewart and Mallon \(2018\)](#), shares similarities with SAM-PK-5265. These include the shape of the frontal and the frontoparietal suture, the position of the pineal foramen and the broadness of the anterior portion of the parietal bar.

The shape of the supratemporal fenestrae in the *Tylosaurus proriger* specimen is square anteriorly and is more triangular posteriorly with pointed posterolateral corners. This is consistent with the shape of the supratemporal fenestrae in *T. pembinensis* figured by [Bullard and Caldwell \(2010\)](#). The anterior margins of the supratemporal fenestrae, nor the frontoparietal suture of SAM-PK-5265 resemble those of *Taniwhasaurus antarcticus* figured by [Fernandez and Martin \(2009\)](#).

The parietal table is relatively broad across the center of the pineal foramen with a maximum width of approximately 105 mm. Ratios of frontal width to parietal width (F:P) for several mosasaur taxa are highlighted in [Table 2](#). The results from [Table 2](#) indicate that SAM-PK-5365 has an F:P of 2.83. This value is equally close to the values calculated for *Prognathodon solvayi* (R033) and *Tylosaurus proriger* (CNM 1862), which both have a F:P of 2.95. *T. bernardi* (R0023) also did not differ widely with a F:P of 3.01, followed closely by *Mosasaurus lemnierii* at 3.06. The results suggest that the SAM-PK-5265 parietal bar is much wider relative to the frontal than that of *Taniwhasaurus antarcticus*, which has a F:P of 5.26.

The fragmentary nature of this element makes it difficult to determine whether the lateral edges of the parietal table were curved as in *Tylosaurus bernardi* ([Jiménez-Huidobro and Caldwell, 2016](#)) or were convex as in *T. proriger* ([Russell, 1967](#); [Jiménez-Huidobro and Caldwell, 2016](#)). However, the lateral edges were not straight as the right anterolateral edge of the parietal table curves medially. Contrary to [Broom's \(1912\)](#) interpretation, the middle section of the parietal bar, where the break occurred, does not show any evidence that it may have become convex, forming a bulbous feature as in *T. proriger* or *T. pembinensis*.

3.3 Postorbitofrontals

The right postorbitofrontal is more complete than the left postorbitofrontal and is visibly attached to the posterior and posterolateral sides of the frontal bone ([Figure 2A](#)). Only a small fragment of the anterior process and dorsal process of the left postorbitofrontal is visible in dorsal view ([Figure 2A](#)). On the ventral surface the postorbitofrontals are sutured to the frontal ([Figure 2B](#)). A small portion of the left postorbitofrontal appears to have been broken off anteriorly on the ventral surface as more of the postorbitofrontal excavation ([Lingham-Soliar, 1992](#)) is visible on the left lateral of the ventral skull ([Figure 2B](#)). Anterior to the left postorbitofrontal excavation, the prefrontal excavation is visible but only a small part of this is visible on the right due to a large fragment of bone missing from the middle-right of the frontal.

3.4 Posterior dentary fragment

The posterior left dentary fragment has a total length of 119 mm and a maximum width of 44 mm ([Figures 3A–C](#)). It has only two and a half tooth positions preserved and there are no functional or replacement teeth present in this dentary fragment. The anterior-most tooth socket has a posterolingually positioned resorption pit associated with it ([Figure 3C](#), black arrow), supporting its mosasaurid origin ([Wiffen, 1980](#)). The smooth appearance of the fossil suggests that it may have been exposed to a tidal environment where it experienced water-weathering. The overall preservation is poor, and the fragment is of little taxonomic value.

Discussion—[Broom \(1912\)](#) noted that the suture between the postorbital and the frontal bone was like that of *Tylosaurus proriger* but that the frontoparietal suture is more like that of *Mosasaurus horridus*, which was later reassigned to *Mosasaurus missouriensis* ([Russell, 1967](#)). Only the frontal

TABLE 2 The ratios of frontal (F) to parietal table (P) width of the different mosasaur taxa including SAM-PK-5265. Measurements were taken at RBINS and from publications cited. The frontal width was measured between the posterolateral edges of the frontal and the parietal width was measured across the posterior-most section of the parietal bar.

Species/specimen	F width (mm)	P width (mm)	F:P	References
SAM-PK-5265	297	105	2.83	Personal Observation
<i>Mosasaurus lemnierii</i> (R0369)	150	49	3.06	Personal Observation
<i>Prognathodon solvayi</i> (R0033)	168	57	2.95	Personal Observation
<i>Tylosaurus proriger</i> (CMN 8162)	~130	~44	2.95	Stewart and Mallon, (2018)
<i>Taniwhasaurus antarcticus</i> (holotype IAA 2000-JR-FSM-1)	~163	~31	5.26	Fernandez and Martin, (2009)
<i>Tylosaurus pembinensis</i> (MM V95)	~289	~71	4.07	Bullard and Caldwell, (2010)
<i>Plioplatecarpus houzeaui</i> (R0136)	167	43	3.88	Personal Observation
<i>Tylosaurus bernardi</i> (R0023)	~226	~75	3.01	Personal Observation

portion of the postorbital is preserved and Broom (1912) suggested that it agreed closely with *T. proriger*, though it was more slender. He also indicated that the broad upper surface of the parietal was exactly as it is in *T. proriger*, but that the pineal foramen sat behind the plane that passes through the front of the [superior] temporal fossa, which differs from the position of the pineal foramen in *T. proriger*. This led Broom (1912) to propose a different species within the genus *Tylosaurus*, and he named this holotype *Tylosaurus capensis*. Lingham-Soliar (1992) suggested that *T. capensis* was more closely related to *Tylosaurus nepaeolicus* rather than *T. proriger*, since the pineal foramen is positioned behind the frontoparietal suture in *T. capensis* and *T. nepaeolicus*, whereas it is positioned on the frontoparietal suture in the later form of *T. proriger* (Lingham-Soliar, 1992). The position of the pineal foramen was long considered a diagnostic feature for species recognition in mosasaurs (Lingham-Soliar, 1992). However, Jiménez-Huidobro and Caldwell (2016) found that the frontoparietal suture shape can vary through ontogeny and between adult individuals, as well as among different species of tylosaurines.

Jiménez-Huidobro (2016) provided the first thorough description of the SAM-PK-5265 dentary fragments and suggested that *T. capensis* be reassigned to the genus *Taniwhasaurus* based on facets and grooves in the crowns of two replacement teeth in the anterior dentary fragment. Furthermore, Jiménez-Huidobro (2016) noted that the enamel ornamentation is like that of *Ta. oweni* and *Ta. antarcticus* which had not been observed in *Tylosaurus*. The reassignment of the SAM-PK-5265 frontoparietal complex and dentary fragments to *Taniwhasaurus* was published by Jiménez-Huidobro and Caldwell (2019); however, the descriptions provided here suggest an alternative interpretation.

The SAM-PK-5265 frontoparietal complex (Figure 2) possesses a number of the key diagnostic characters of the genus *Prognathodon*. SAM-PK-5265 frontoparietal complex has a short, triangular frontal that is only slightly longer than wide. The lateral edges of the frontals are almost straight, with a slight outward bulge posteriorly, which is also evident in the diagram of the *P. overtoni* specimen (TMP 2007.034.0001) from the lower Bearpaw Formation, southern Alberta, Canada (Konishi et al., 2011, p.1030). Portions of the postorbitofrontals are visible lateral to the frontal as in *P. overtoni* (Konishi et al., 2011).

Konishi et al. (2011) detailed the medial expansion of the anterior prefrontals of the *P. overtoni* specimen (TMP 2007.034.0001) resulting in the anterior tip of the frontal to be narrow and preventing the external narial openings from invading the anterior of the frontal. Similarly, with the SAM-PK-5265 frontoparietal complex, there is no evidence to suggest that the internarial bar overlapped the frontal or that the frontal contributed to the shape of the posterior external narial openings,

which is diagnostic of *Prognathodon* (except for in *P. saturator* and in *P. currii*). Therefore, it is suggested that the anterior tip of the frontal bone in SAM-PK-5265 is broken and thus was probably not as broad as was previously interpreted. Its smooth and rounded appearance may be an artifact of taphonomy and weathering.

The frontoparietal suture is sinusoidal and the medial sutural flanges of the frontal broadly enclose the anteromedial portion of the parietal surface (see Figure 2), which is diagnostic for *Prognathodon* (except *P. saturator*). The median sutural flange forms a crest directly anterior to the pineal foramen (Figure 2), which is unusual in mosasaurs.

Unlike in the generic diagnosis (Konishi et al., 2011), the frontoparietal complex (SAM-PK-5265) does not possess a dorsal midline keel or the grooves in the surface behind the keel; the posterolateral edges of the frontal bone are rounded and blunt and are not wing-like, and the parietal postorbital processes are short and do not reach the posterolateral corner of the frontal. However, the bone is not well-preserved, and these delicate features are likely prone to post-mortem destruction and weathering.

There are some shared characteristics between the SAM-PK-5265 frontoparietal complex and those of *Ta. antarcticus*, which could indicate why a phylogenetic analysis of the tylosaurine mosasaurs placed “*T. capensis*” as a sister taxon to *Ta. antarcticus* (Jiménez-Huidobro and Caldwell, 2019). The posterolateral corners of the frontal bone, as well as the nearly straight posterolateral sides of the frontal, are like those of *Ta. antarcticus*, although the frontoparietal sutures differ (Fernandez and Martin, 2009). Furthermore, two characteristics that are supposedly present in all tylosaurines (Jiménez-Huidobro and Caldwell, 2019) are not present in the frontoparietal complex (SAM-PK-5265). These features are 1) external nares invading the frontal, and 2) internarial bar overlapping the anterior tip of the frontal.

The posterior dentary fragment (Figure 3) is of little diagnostic value because there is a lot of bone missing from the anterior and posterior ends of the fragment, as well as from the ventral surface. Furthermore, the dentary fragment contains no teeth and appears to be weathered. This caused the loss of most of the surface detail on this fragment. However, the size and shape of the tooth sockets can be determined (Figure 3A). These are large (~430 mm) and rounded and are like those visible in the maxillae of the muzzle unit as well as the tooth bases of IT-1 and IT-2.

cf. PROGNATHODON Dollo, 1889 (Figures 4–7)

Specimen and location—CGP/1/2265, a large, robust muzzle unit from southwest of the Mzamba River, Pondoland, Eastern Cape, SA.

Remarks—Specimen CGP/1/2265 (Figures 4–7) was rediscovered in the Geoscience Museum collections in Pretoria, SA by one of us (AC). Preparation at the Iziko South African Museum in 2019 revealed a set of upper jaws with other articulated elements forming a muzzle unit. Two isolated fragmentary teeth were also removed from the matrix around

the muzzle unit during preparation. It was speculated that this specimen may be the “[*Mosasaurus*] lower jaw” that Rogers and Schwarz (1902, p.41) referred to in their report and thus is associated with SAM-PK-5265 (Chinsamy-Turan et al., 2018). A fragmentary isolated shark tooth was found in the matrix surrounding the muzzle unit (*Squalicorax pristodontus*).

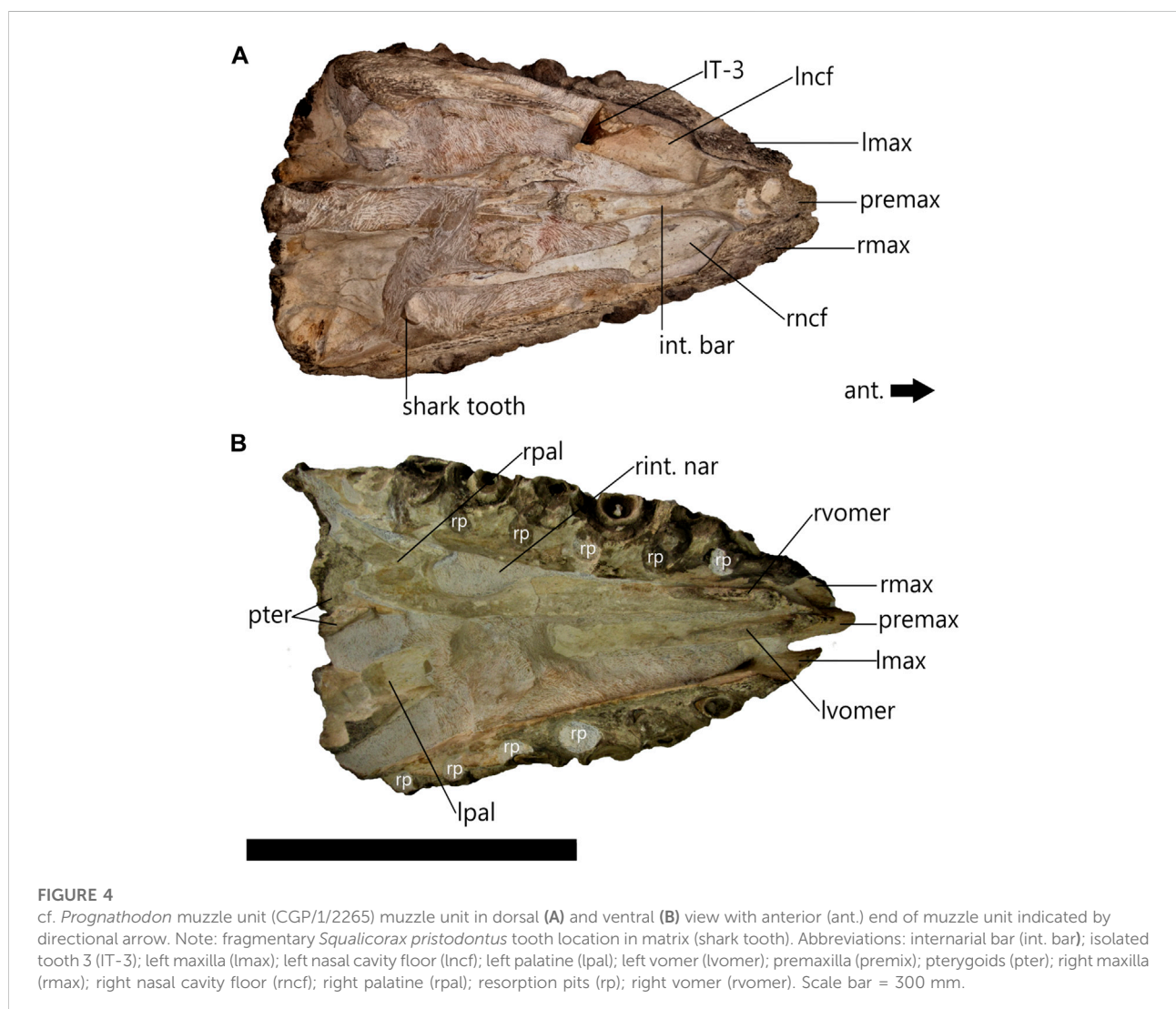
Description—This specimen is comprised of attached cranial elements, which would make up most of the anterodorsal muzzle unit (Russell, 1967) including the maxillae, premaxilla, vomers, palatines, pterygoids and a few teeth (Figures 4, 5). This cranial unit has a total length of approximately 550 mm, but due to the incompleteness of the skull, it is impossible to estimate the full skull length. The overall preservation is good; however, the external surfaces are not as well-preserved as the internal surfaces of the skull elements (Figures 4A,B). The better-preserved bones and

teeth are those that were embedded in the matrix and only exposed during preparation.

Preparation of the ventral surface revealed the palate and the distortion of the skull that likely occurred during post-mortem decomposition and fossilization (Figure 4B). It appears that it had been mediolaterally compressed during the fossilization process causing the left side of the skull to collapse and the skeletal elements to become displaced (Figure 4B). The left ventral side is not as well preserved as the right, nor was it prepared as fully.

3.5 Maxillae

The left maxilla is 505 mm long and the right maxilla is 550 mm long. Neither the right nor left maxillae are complete. The tooth-



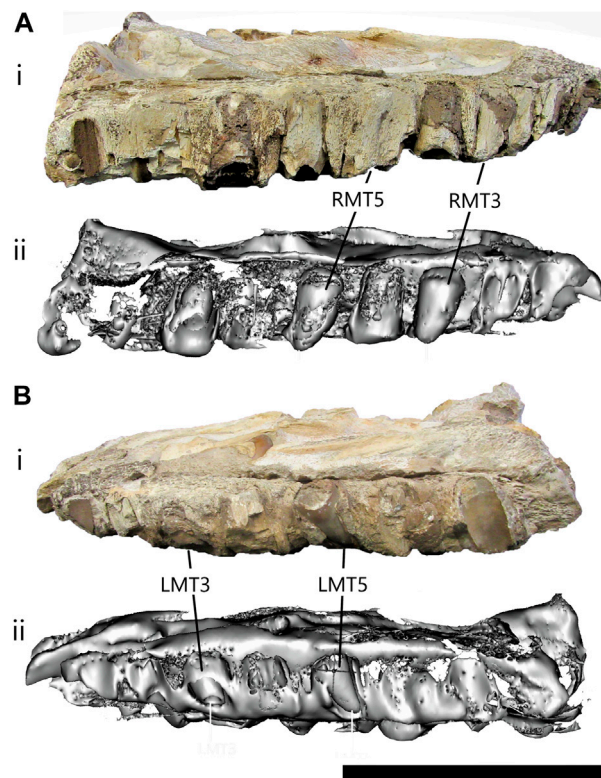


FIGURE 5

cf. *Prognathodon* muzzle unit (CGP/1/2265) in right lateral view (A) and left lateral view (B) photographs (i) and CT scans (ii) of the CGP/1/2265 muzzle unit. No functional teeth present in maxilla, but tooth sockets have been infilled presenting mould of third (RMT3) and fifth (RMT5) right maxillary teeth, and third (LMT3) and fifth (LMT5) left maxillary teeth. Right side has 9 maxillary tooth positions, third and fifth are not visible except on CT scan. Left side has 7 maxillary tooth positions, third only visible on CT scans, but fifth visible externally as maxilla has broken away. Scale bar = 200 mm.

bearing regions of the maxillae are preserved, although the facial elements, i.e., the thin, flat part of the maxilla that encloses the lateral sides of the face, are both lost thus exposing the left and right nasal cavity floors (Figure 4A). This is likely because the facial elements are more delicate (personal observation made at the RBINS) and therefore more likely to break off during fossilization. In addition to this, the lateral sides of the tooth-bearing elements are incomplete (Figures 5Ai, Bi). The lateral portion of the right maxilla also appears to have undergone some surface weathering. The replacement teeth and tooth sockets are not completely exposed, as on the left (Figure 5Bi), but this prevented observation of any foramina that may have been present on this surface (Figure 5Ai).

Anteriorly, the maxillae are both mediolaterally compressed and become wider posteriorly to accommodate the teeth (Figure 4). The maxillae are not in line as the anterior tip of the left maxilla has been broken off, although the right maxilla is almost in line with the anterior tip of the premaxilla. Dorsally the anteromedial side of the right maxilla is in contact with the right lateral side of the premaxilla (Figure 4A). However, the left maxilla and premaxilla are not in contact (Figure 4B) as it

appears that some of the left maxilla had broken off near this contact and the bones had shifted during taphonomic processes.

In ventral view the resorption pits are positioned posterolingual to the functional teeth/tooth sockets and are infilled (Figure 4B). Anteriorly, the right vomer is in contact with, but not sutured to the right maxilla and presents a distinct vomerine aperture; this contact is broken at the anterior margin of the right internal narial opening (Figure 4B). Posteriorly, the right palatine contacts the right maxilla. Due to the displacement of some of the cranial elements during fossilization, there are no bones in contact with the medial surface of the left maxilla; therefore, the smooth and straight medial surface is visible (Figure 4B).

Nine tooth positions are visible in the right maxilla and seven tooth positions are visible in the left maxilla (Figure 5). All the functional and replacement maxillary teeth are missing and had likely fallen out of the tooth sockets during decomposition. Some of the tooth sockets had then been infilled with sediment leaving moulds of the replacement

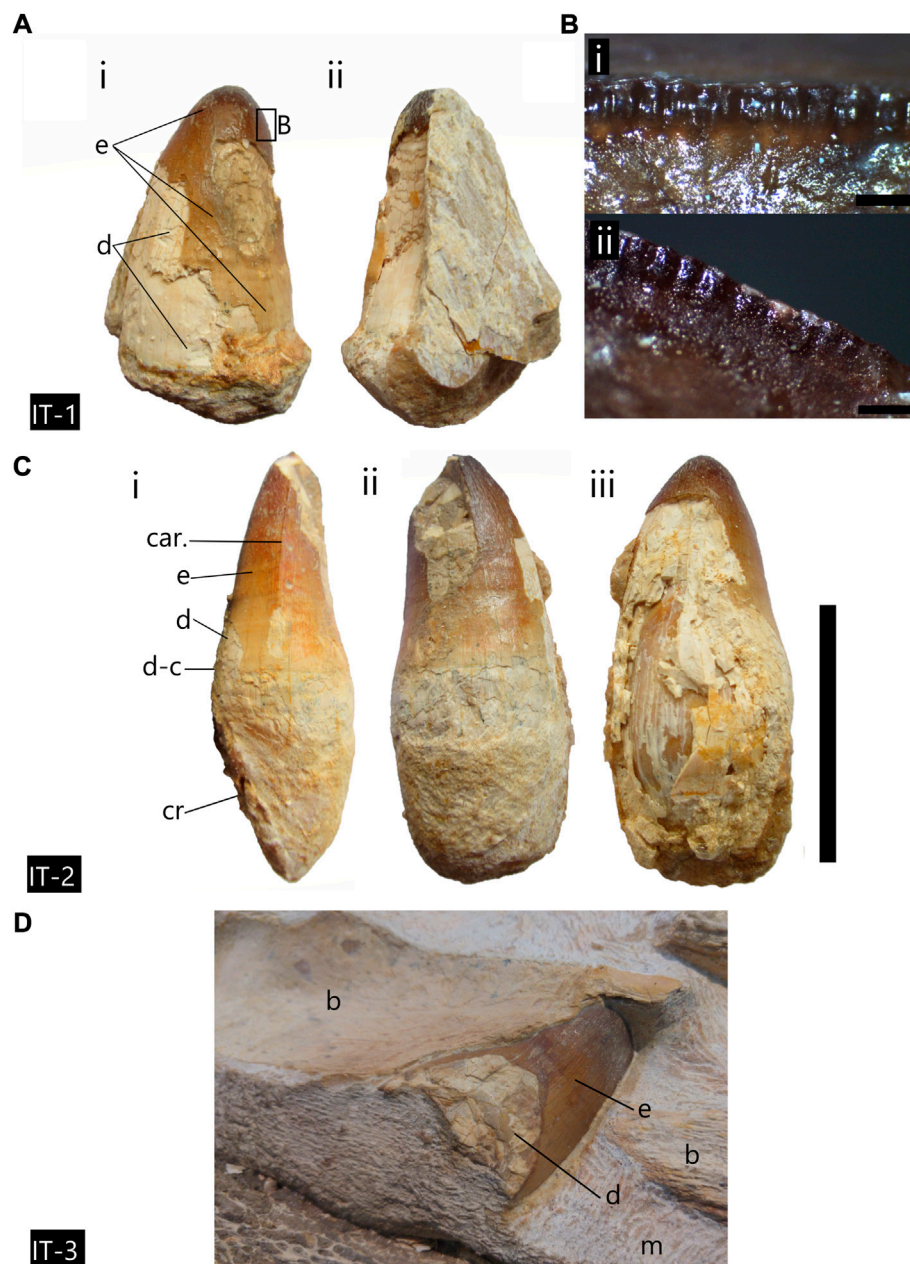


FIGURE 6

Fragmentary, isolated teeth, from cf. *Prognathodon* muzzle unit (CGP/1/2265). (A) Isolated tooth 1 (IT-1) in (i) labial and (ii) lingual view. Only enamel crown present. Enamel and dentine portions indicated. (B) IT-1 fine serrations visible on anterior and posterior carinae. (C) Isolated tooth 2 (IT-2) in (i) posterior, (ii) lingual and (iii) labial view. (D) Isolated tooth 3 (IT-3) partially visible, wedged beneath nasal cavity floor bone and surrounded by matrix. Abbreviations: car., posterior carinae; e, enamel; d, dentine; d-c, dentine-cementum contact; and cr, cementum root is indicated. Scale bars (A) = 50 mm; (Bi) = 1 mm, (Bii) = 0.5 mm; (C) = 90 mm; (D) = no scale.

teeth that are visible with CT scans (Figure 5Aii, Bii). One of these replacement tooth moulds is visible externally in the left maxilla, LMT5 (Figure 5Bi). The moulds of the replacement teeth show that they are large and bulbous with blunt apices and are posteriorly recurved.

3.6 Premaxillae

The premaxillae are fragmentary, and the posterior and anterior-most portions are missing (Figure 4). This is unfortunate because many diagnostic characters of the

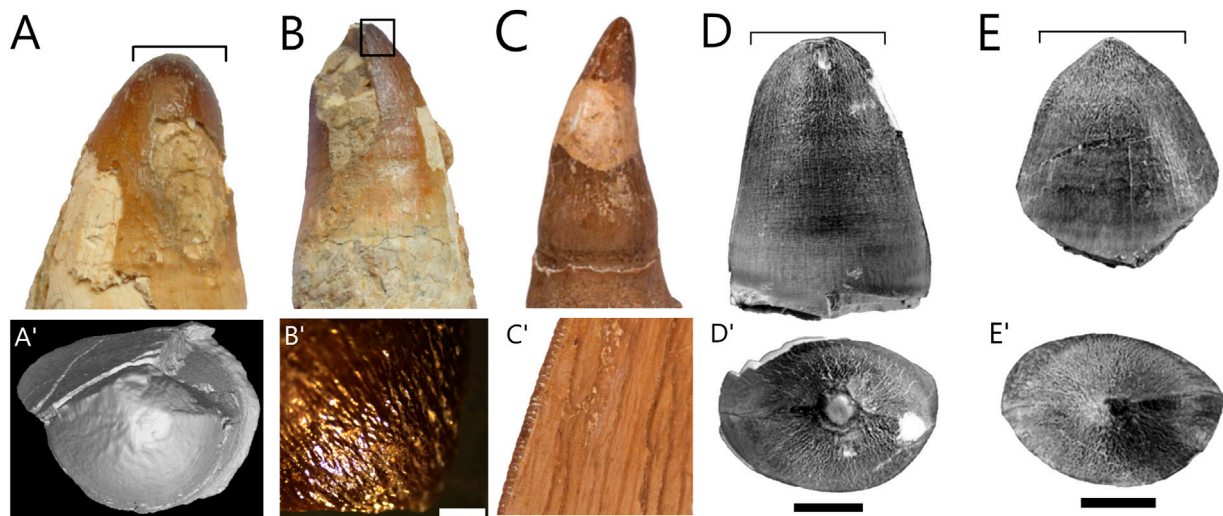


FIGURE 7

Micro-CT scans of fragmentary, isolated teeth, from cf. *Prognathodon* muzzle unit (CGP/1/2265). (A) Isolated tooth 1 (IT-1) in labial view. (A') Three-dimensional micro-CT scan image of IT-1 in occlusal view with blunt apex and anastomosing ridges visible. (B) Isolated tooth 2 (IT-2) in lingual view with box frame giving locational information for B'. (B') High magnification image of anastomosing ridges at apical region of IT-2 using dissecting microscope. (C) Photograph of CCMGE 818 *P. lutugini* tooth crown in lingual view adapted from Gregoriev (2013). (C') High magnification image of fine serrations on carinae of *P. lutugini* adapted from Gregoriev (2013). (D) Photograph of OCP. DEK/GE 349 "*P. currii*" tooth crown in labial or lingual view adapted from Bardet et al. (2005). (D') Photograph of OCP. DEK/GE 349 "*P. currii*" tooth crown in occlusal view adapted from Bardet et al. (2005). (E) Photographs of OCP. DEK/GE 350 "*P. currii*" tooth in labial or lingual view adapted from Bardet et al. (2005). (E') Photographs of OCP. DEK/GE 350 "*P. currii*" tooth in occlusal view adapted from Bardet et al. (2005). Scale bars: (A,A',B,C,C') = not to scale; B' = 2 mm; (D,D',E,E') = 10 mm.

posterior margins of the external nares and the anterior tip and premaxillary teeth are lost (Figure 4). The total length of the incomplete premaxilla is 278 mm. In the lateral view the anterior tip of the premaxilla is rectangular and has a slight ventral curvature (Supplementary Figure S1).

In dorsal view, it resembles a broken arrowhead (Figure 4A). It is the main contributor to the internarial bar, which separates the two external narial openings on the top of the head. It narrows posteriorly to form the internarial bar, which has a smooth surface and a minimum width of approximately 14 mm, which would likely be the widest part of the external narial openings. It then slightly widens posteriorly again so that the most posterior end of the internarial bar bulges both laterally and dorsally (Figure 4A).

3.7 Vomer-palatine complex

Both left and right vomeropalatines are present and relatively well-preserved. The right side is better preserved than the left with the right pterygoid in contact with the posterior region of the palatine and the posterolateral palatine buttressed against the medial maxillary wall (Figure 4B). With respect to the vomers, the anterior half of the right vomer is in contact with the anterior maxillary wall

enclosing the internal narial openings. The whole ventral right side was fully prepared exposing a large area between the vomer-palatine suture and the square body of the left palatine (Figure 4B); the anterior ramus of the left palatine is not visible as that portion was not prepared.

The vomers are elongated bones that span more than half of the anterior portion of the palate (Russell, 1967). The left vomer in CGP/1/2265 has been displaced from its original position in the skull and now lies beneath the internarial bar of the premaxilla (Figure 4B). The right vomer is complete, apart from a small piece missing from the anteroventral surface but it is in its original position and is 254 mm long. The vomers are both mediolaterally compressed and narrow anteriorly in ventral view (Figure 4B). Both the left and right vomers have a process that runs along the anterolateral sides of the ventral surface. The process on the right vomer appears as though it has been broken off towards the posterior end. On the left vomer there is a well-preserved crest that is approximately 185 mm in length.

The palatines in CGP/1/2265 are large with the maximum length of the right palatine from the vomer-palatine suture to the posteromedial point being approximately 187 mm. The vomers and palatines are dorsoventrally thickened and robust, much like the rest of the muzzle unit. The main bodies of the palatines are relatively square in shape with a scooped floor behind the internal narial openings forming the curved roof of the mouth

(Figure 4B). The anterolateral process of the palatine is short and therefore allows the medial maxillary wall to play a greater role in shaping the internal narial openings. The posterior boundary of the right internal narial opening is smooth and rounded (Figure 4B).

The elongated anterior process of the palatine gradually narrows anteriorly to a minimum width of 19.61 mm, to form a rounded medial surface of the internal narial opening and then widens slightly to meet the vomer at the vomer-palatine suture (Figure 4B), which is at least 33.32 mm wide and is shaped like a shallow 'V' (Supplementary Figure S2). The right vomer-palatine clearly overlaps the palatine and even has small flanges on the posterolateral corners (Supplementary Figure S2, black arrowheads). Although it is partially covered by matrix, the posterior border of the left vomer is visible and appears to be identical in shape to the posterior border of the right vomer (Supplementary Figure S2, grey lines). The anterior ramus of the right palatine is not visible and may be covered by matrix or is missing (Supplementary Figure S2).

3.8 Pterygoids

Only the anterior parts of the pterygoids are preserved (Figure 4). Unfortunately, the tooth-bearing elements and teeth, as well as the elements at the posterior end of the pterygoids such as the basisphenoid processes, ectopterygoid processes, and quadratic rami are all lost.

The anteromedial process of the right pterygoid is in its life position and is tightly buttressed against the medial side of the palatine body (Supplementary Figure S3, grey dashed line). The anteromedial process of the left pterygoid is unnaturally overlying the right due to the taphonomic displacement of the left cranial bones (Figure 4B). These processes are both relatively long, the right is at least 88.35 mm in length and the left is 64.81 mm. The left appears to be dorsoventrally deep. Both anteromedial processes are pointed at the anterior tip. (Supplementary Figure S3). There is an anterolateral process of the pterygoid bone that is shorter and rounded, and anteriorly contacts but is not fused to the posterior surface of the right palatine body (Supplementary Figure S3, black arrow).

3.9 Isolated teeth

There were two isolated fragmentary teeth (IT) (Figures 6, 7) extracted from the matrix around the anterodorsal muzzle unit during preparation (IT-1 and IT-2). These isolated teeth are like the replacement tooth LMT5 (Figure 5B), and it is assumed that they belong to the same individual. The first isolated tooth, IT-1 (Figures 6A,B) was extracted from the matrix near the middle of the palate. The second isolated tooth, IT-2 (Figure 6C) was extracted from the left side of the dorsal surface near the

posterior region of the internarial bar. Another isolated tooth, IT-3, was also found during preparation; however, this one is wedged beneath what appears to be the bone forming the floor of the nares (Figure 6D). It was not removed due to the potential damage that its removal could cause to this region of the skull.

IT-1 (Figures 6A,B) is the most fragmentary of the two extracted isolated teeth. It has a mostly complete enamel crown measuring approximately 46 mm in length, but the cementum root is absent. Much of the enamel has flaked off the tooth. The isolated teeth are posteromedially recurved as in Figure 6Ci. The carinae on IT-1 and IT-2 are finely serrated (Figure 6B), which is only observed with a hand lens or microscope. These serrations form an ornamented enamel ridge along the carinae (Figure 6B), have a globular appearance, and are approximately uniform in shape and size (Figure 6B).

IT-2 (Figure 6C) is better preserved and more complete in the sense that it has both the enamel crown and cementum root attached, indicating that it is a functional tooth or a late-stage replacement tooth. IT-2 is anatomically and taxonomically valuable, and thus was not chosen for destructive analysis. A portion of the apex is missing from the labial side of the tooth. The enamel crown is approximately 47 mm in length and the cementum root is approximately 39 mm in length.

The two extracted isolated teeth (IT-1 and IT-2) have enamel crowns that are subconical in shape. The bases of the enamel crowns are bulbous and about circular. Both teeth possess anterior and posterior carinae. They become more elliptical towards the apices as the teeth become slightly labiolingually compressed and the carinae become more pronounced (Figures 6A,B). The enamel on these two teeth is smooth and there is no evidence of grooves or facets (Figures 6A,B). The enamel near the apical regions of the teeth does appear to be rougher and small anastomosing ridges are visible (Figures 6A,B).

Discussion—The size and robustness of the muzzle unit indicate an overall massive skull. The maxillae are large with mediolaterally thick tooth-bearing parts to accommodate the heavy dentition. The massive nature of the skull elements of this specimen agrees with the massive nature of elements present in the mosasaurine genus *Prognathodon*. A maximum of 9 teeth were counted in the right maxilla, but anterior and posterior portions of both maxillary bones are missing. It is likely that the complete maxillae could have held 3–4 more teeth, therefore meeting the 12–13 maxillary teeth criterion for *Prognathodon*.

The isolated teeth are very similar to those seen in some *Prognathodon* species. They are unlike the teeth of *P. solvayi* (R033), which are sharper, more medially recurved, and quite strongly faceted (personal observation of specimens at RBINS). However, they are more similar to the teeth of *P. giganteus* (R106), which have smooth enamel surfaces, anterior and posterior carinae, and fine serrations on the carinae of two replacement teeth are similar to *Prognathodon* as characterized by Konishi et al. (2011). At the same time, *P. giganteus* teeth are labiolingually flattened, anteroposteriorly

wide, less globular and slightly sharper than IT-1 and IT-2. Grigoriev (2013) figured teeth belonging to *P. lutugini* (previously *Dollosaurus lutugini*) from Campanian deposits of Eastern Ukraine, which also resemble those of CGP/1/2265 in that they are bicarinate with fine serrations and have the same wrinkled enamel texture towards the apical regions of the teeth (Figure 7B', C'). However, like those of *P. solvayi*, *P. lutugini* teeth appear to be more recurved and sharper than IT-1 and IT-2 (Figure 9C).

The isolated teeth of CGP/1/2265 appear most like two tooth crowns (OCP.DEK/GE 349 and OCP. DEK/GE 350) from the Maastrichtian of Morocco, which were assigned to *P. currii* (Bardet et al. (2005) (Figures 7D,E). The similarities include a subconical shape; a slightly swollen basal crown that is elliptical in cross-section; well-developed anterior and posterior carinae that are serrated; lingual and labial surfaces are subequal in size (compare Figure 7A' and E'); enamel approximately 0.5 mm thick, particularly at the apex of the tooth giving it a darker colour (see Figures 6A,B); unfaceted and smooth enamel except for the upper two-thirds of the crown that have crude anastomosing ridges (Figure 7A', B'). Differences include the fact that *P. currii* teeth have straight tooth crowns (Bardet et al., 2005), whereas IT-1 and IT-2 have a slight posteromedial recurvature. There is also a small sharp point at the apex of OCP. DEK/GE 350 tooth crown (Figure 7E, E') that is not visible on OCP. DEK/GE 349, probably due to wear (Figure 7D'). The apex of IT-2 is missing, but Figure 7A' shows IT-1 in occlusal view and there seems to be a similar tooth wear pattern at the apex. IT-1 has been identified as a replacement tooth thus one would not expect to find evidence of wear. However, it is possible that the sharp point on the apex of IT-1 was worn down if it was exposed.

There are concerns regarding the assignment of the CGP/1/2265 to *P. currii* based on the isolated teeth. The *P. currii* type specimen has no complete or well-preserved tooth crowns, and the dentition has been largely described from reconstructions (Christiansen and Bonde, 2002). Therefore, despite the similarities shared between the isolated teeth of CGP/1/2265 and the teeth figured by Bardet et al. (2005), the assignment of the two tooth crowns from Morocco (OCP.DEK/GE 349 and OCP. DEK/GE 350) to *P. currii* is equivocal and needs to be treated with caution. IT-1 from the CGP/1/2265 muzzle unit dates to the End Maastrichtian using strontium isotope dating (see Section 4). The CGP/1/2265 isolated teeth are thus assigned to cf. *Prognathodon*.

3.10 Associated shark tooth—*Squalicorax pristodontus*

Description—The shark tooth is directly associated with the CGP/1/2265 muzzle unit (Figure 8) It is located on the dorsal right side of the muzzle unit towards the posterior end (see Figure 4A).

Only the apical region of the tooth crown is covered with a thin enamel layer. However, the shape of the entire tooth is visible (Figure 8). It has a bilobate root. The maximum width across the root-crown boundary is approximately 25 mm. The tooth is wider than it is long from the root to the apex. There is no evidence to indicate the presence of cusplets on the tooth (Figure 8). The crown has a crescentic shape with a bulbous mesial side. The distal side has a concave edge towards the apex. Along the edges of the crown are well-developed fine serrations, which are visible more clearly on the distal side (Figure 8). The serrations seem to have worn slightly on the medial side of the tooth near the apex. No fine striations or grooves are visible on the tooth surface.

We have identified the isolated shark tooth found associated with the CPG/1/2265 muzzle unit (Figure 8) as belonging to the extinct shark species, *Squalicorax pristodontus*. *Squalicorax* is an extinct genus of the Anacoracidae family (Order: Lamniformes), the fossils of which are common in Cretaceous deposits around the world (Compagno, 1990; Shimada and Cicimurri, 2005). Remains were found in North America, South America, Australia, Asia, Europe, and Africa (Shimada and Cicimurri, 2005). Furthermore, remains of mosasaurs and *Squalicorax* sharks were also found together previously (e.g. Dortangs et al., 2002; Chin et al., 2008; Konishi et al., 2011; Konishi et al., 2014).

Gottfried and Rabarison (2001) figured and described *Squalicorax pristodontus* teeth from the Late Cretaceous and Paleocene deposits of the Mahajanga Basin in north-western Madagascar, indicating that these sharks were present around Southern Africa at this time. They described the same fine serrations, bulbous mesial side and a crescentic shape that is noted in the CGP/1/2265 isolated shark tooth (Figure 8).

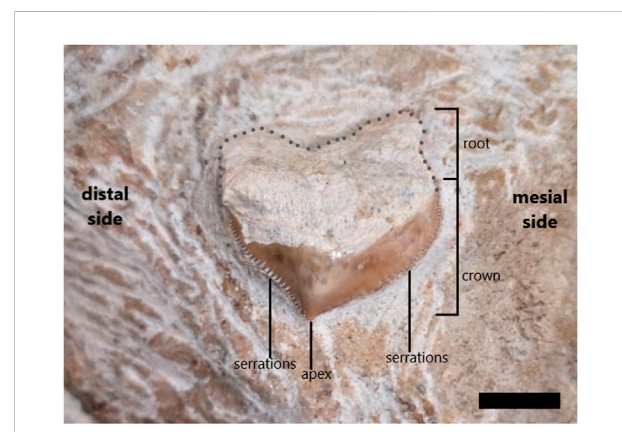


FIGURE 8
Squalicorax pristodontus tooth (from CPG/1/12,265) found in matrix surrounding cf. *Prognathodon* muzzle unit prior to removal of some enameloid for comparative purposes. Root and enameloid-covered crown are indicated, as well as well-developed serrations on mesial and distal side of tooth. Dotted line reconstructs root base, which is not clear as near to basal region of tooth due to missing enameloid. Scale bar = 10 mm.

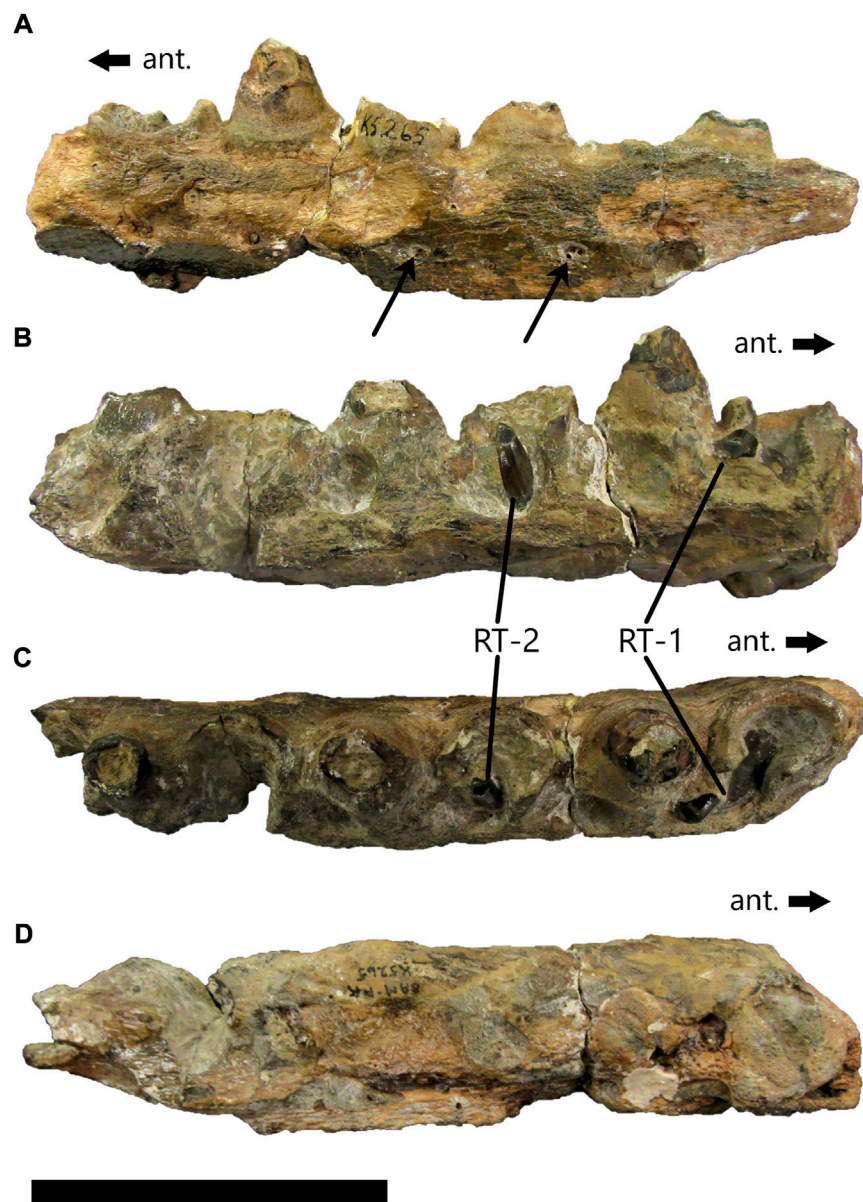


FIGURE 9

Anterior dentary fragment, cf. *Taniwhasaurus* (SAM-PK-5265) in lateral (A), medial (B), dorsal (C) and ventral (D) view. Thin black arrows in (A) indicate large foramina. Two replacement teeth are indicated in (B) and (C). Directional arrows show anterior end of fragment. Scale bar = 100 mm.

The isolated *Squalicorax pristodontus* tooth figured by [Chin et al. \(2008, Figure 5C, p.2680\)](#) is very similar to that which was found in the matrix around the muzzle unit. [Shimada and Cicimurri \(2005\)](#) also figured several teeth belonging to various species of the *Squalicorax* genus and their drawing of the *S. pristodontus* tooth, as well as the estimated temporal range of the species, from Early Campanian to the Late Maastrichtian ([Shimada and Cicimurri, 2005, Figure 1, p.242](#)), supports the identification the CGP/1/2265 isolated shark tooth as *S.*

pristodontus.

TYLOSAURINAE Williston, 1897

cf. TANIWHASAURUS Hector, 1874 (Figures 9–11)

Diagnosis—for an emended diagnosis, see [Caldwell et al. \(2008\)](#).

Specimen and location—SAM-PK-5265 Anterior Dentary Fragment from the Cretaceous rocks southwest of the Mzamba River, Pondoland, Eastern Cape, SA ([Rogers and Schwarz, 1902](#))

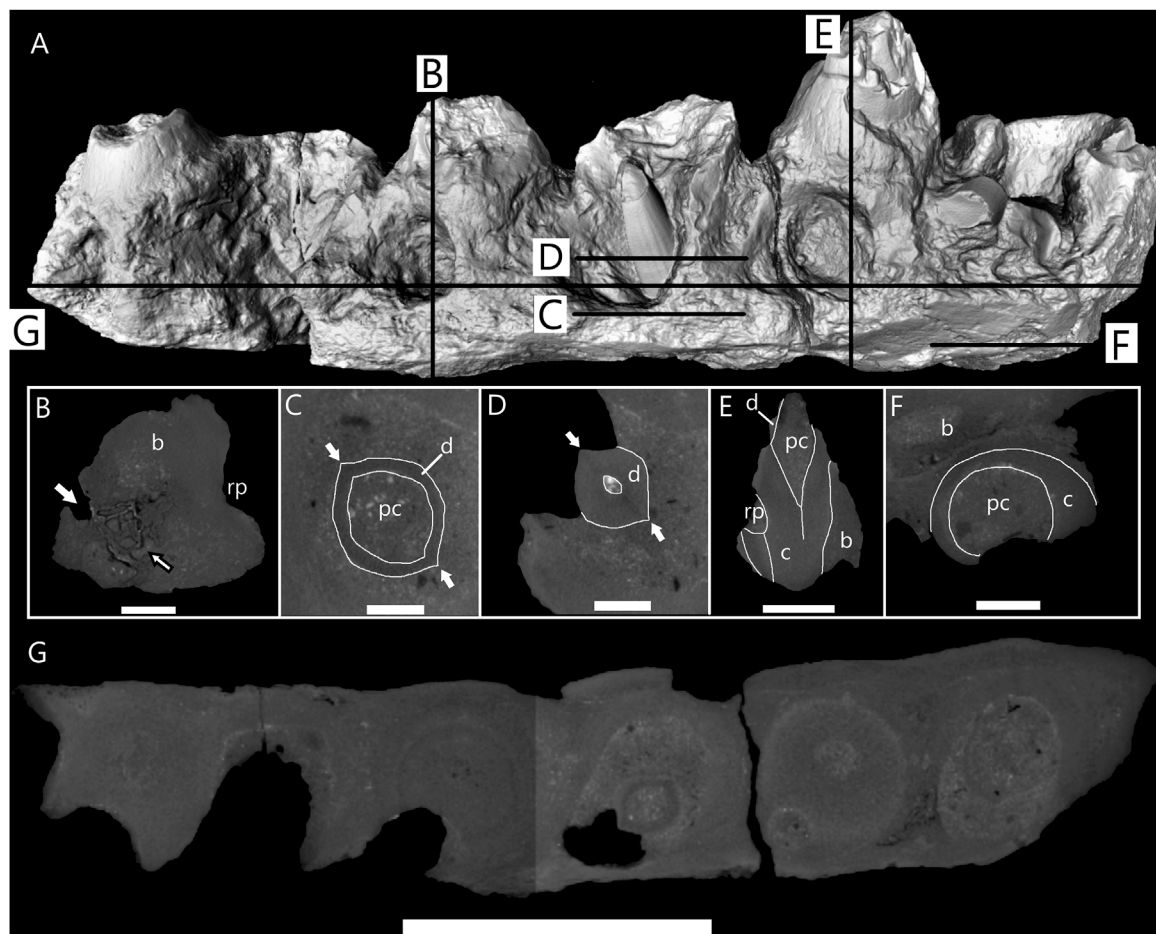


FIGURE 10

Micro-CT scan images of anterior dentary fragment of cf. *Taniwhasaurus* (SAM-PK-5265). **(A)** Three-dimensional micro-CT image of anterior dentary fragment with lines to indicate location of sections shown in B–G. **(B)** Longitudinal section through fragment at position of fourth functional tooth position showing resorption pit on medial side and one foramina (white arrow) on distal side. Black outlined arrow points to unusual bone tissue next to foramen. **(C)** Horizontal section through dentary showing base of second replacement tooth (RT-2) crown. It is ovate shape with two distinct carinae (white arrows) and large pulp cavity. **(D)** Horizontal section through dentary showing cross-sectional shape of RT-2 halfway up crown. Maintains ovate shape with two carinae. Smooth facets are visible on surface of tooth in both horizontal section and three-dimensional image **(A)**. **(E)** Longitudinal section through second functional tooth showing various tooth tissues, discernible by density differences. Pulp cavity infilled with sediment and most of dentine lost. **(F)** Horizontal section taken near ventral surface where cementum of first tooth visible. Suggests significant amount of bone missing from ventral surface of dentary. **(G)** Horizontal section through entire dentary fragment showing each tooth position and visible changes in density between different tissues. Abbreviations: bone tissue **(B)**; cementum **(C)**; dentine **(D)**; resorption pit (rp). Scale bars: **(A, G)** = 50 mm; **(B)** = 10 mm; **(C, D)** = 6 mm; **(E)** = 20 mm; **(F)** = 8.5 mm.

Description—This specimen is a partial left dentary fragment (Figures 9–11), which was determined to be from the anterior portion of the dentary due to its slenderness and the six large foramina visible on the lateral surface showing a posterodorsal entrance/exit of blood vessels and/or nerves (Figure 9A, arrow). Foramina seem to be present on the anterior half of dentaries in most mosasaurs. Unfortunately, bone is missing from both ends of the dentary, which means that no features of the anterior tip are visible and there is no information regarding the contact with the left splenial, angular, coronoid or surangular on the posterior end. The total length of

the dentary fragment is approximately 200 mm, and the maximum height is approximately 43 mm (from the ventral surface to the bottom of the interdental spaces). However, a significant amount of bone is missing from the ventral surface as is evident from the micro-CT scans of this dentary fragment (Figure 10A) therefore it is impossible to determine the actual height of the dentary. The maximum mediolateral width of the fragment is 39 mm.

There are six functional tooth positions in the anterior dentary fragments, but no complete functional teeth in the fragment (Figures 9–11). The interdental spaces are small and

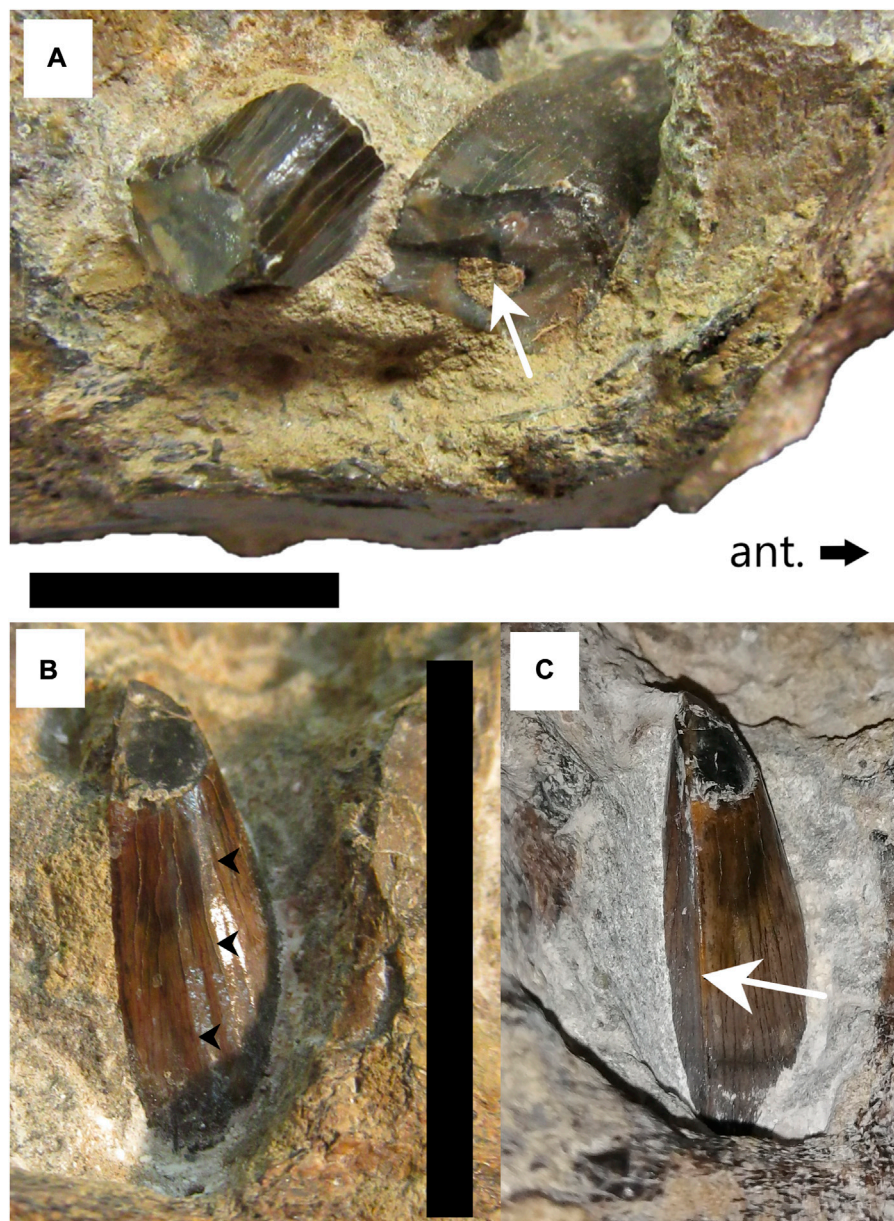


FIGURE 11

Replacement teeth on anterior dentary fragment cf. *Taniwhasaurus* (SAM-PK-5265). **(A)** First broken replacement tooth (RT1) at anterior (ant.) end of fragment. Pulp cavity visible within tooth (white arrow). **(B)** Lingual view of second replacement tooth (RT2) with smooth facets (black arrow heads). **(C)** Posteromedial view of RT-2 after preparation to expose posterior carina (white arrow). Scale bars = 20 mm.

equidistant. There are resorption pits, and two replacement teeth are positioned posterolingually to the fragmentary functional teeth/tooth sockets. The replacement teeth are positioned towards the anterior end of the fragment (RT-1) and in the center (RT-2) (Figures 9B,C). The replacement teeth appear relatively small in comparison to the functional teeth that preceded them (Figures 10B,C), suggesting they had not yet

reached stage 4 of Caldwell's (2007) eight-stage ontogenetic pattern for mosasaur tooth development.

RT-1 is broken, which exposed the small sediment-infilled pulp cavity (Figure 11A, white arrow). It is difficult to determine its cross-sectional shape due to the bone and matrix surrounding it and it appears that the tooth may have been compressed slightly during fossilization. The

enamel surface that is visible is relatively smooth, without any deep striations (Figure 11A).

RT-2 is almost complete and in its upright life-position (Figures 11B,C). The apex of this tooth is broken off obliquely. The enamel is smooth and gentle facets are visible on the medial side (Figure 9B, black arrowheads, 10 A). Further preparation at the Iziko South African Museum allowed for the posterior carina to be observed (Figure 11C, arrow). The posterior carinae are sharp with no serrations visible along their length.

Initially, the anterior carina was not visible as it was covered by bone (Figure 11C), but micro-CT scans revealed the anterior carina as well as the ovate, subconical shape of RT-2 (Figures 10C,D). The enamel layer of RT-2 is thin and is not visible on the micro-CT scans. The enamel facets visible in Figures 10A, 11B are hardly visible in cross-section, indicating that they are very fine (Figure 10D).

Discussion—The dentary fragment itself is of little diagnostic value because there is a lot of bone missing from the anterior and posterior ends of the fragment, as well as from the ventral surface. The remnants of functional teeth and replacement provide more diagnostic information (Figures 10, 11). Micro-CT analysis of SAM-PK-5265 anterior dentary fragment (Figure 10) revealed that the replacement tooth shared some similarities with IT-1 and IT-2 (CGP/1/2265) (see Figure 6). It is subconical in shape, elliptical in cross-section around the midsection (Figure 10C) and it has both anterior and posterior carinae (Figure 10D). However, there are approximately four smooth facets visible along the exposed length of the replacement tooth in the anterior dentary fragment, which are not present on the isolated teeth from the muzzle unit (CGP/1/2265). Furthermore, the apical region of the replacement tooth is missing and therefore it is impossible to assess the shape of the tooth apex, or to detect any anastomosing ridges.

Jiménez-Huidobro and Caldwell (2019) suggested that the SAM-PK-5265 dentary fragments and frontoparietal complex be reassigned to *Taniwhasaurus* based on the faceted enamel of the replacement teeth in the anterior dentary fragment. Through further preparation and micro-CT analysis, this study revealed the presence of unserrated anterior and posterior carinae on the replacement teeth, another feature of *Taniwhasaurus*. However, the enamel ornamentation on the replacement teeth in the anterior dentary fragment does not resemble that of the teeth of *Ta. antarcticus* (Martin and Fernandez, 2007; Fernandez and Martin, 2009) or *Ta. oweni* (Caldwell et al., 2005), which shows strong and deep vertical striations. The facets on the SAM-PK-5265 replacement tooth are smooth, gentle, and not as numerous, making them more like those of *Ta. mikasaensis* from the upper Santonian-lower Campanian of the Island of Hokkaido, Japan (Caldwell et al., 2008).

cf. PLIOPLATECARPINAЕ (Dollo, 1884) Williston, 1897 (Figure 12).

Specimen and location—an indeterminate mosasaurid partial vertebra, recovered by Chris Shelton in 2016 from the Nibela Peninsula St Lucia, KwaZulu-Natal, SA (S 27°59′09.02" - E 39°24′38.1") (Chinsamy-Turan et al., 2018).

Remarks—This specimen currently has not been accessioned into a collection and bears no specimen number. In addition to the remains from Pondoland another indeterminate mosasaurid partial vertebra was recovered from the Nibela Peninsula, St Lucia approximately 355 km north-east of the Pondoland mosasaurid locality (Chinsamy-Turan et al., 2018). The modern Lake St Lucia estuary seen today originated during the mid-Holocene when flood waters carved rivers into the Cretaceous bedrock (Gomes et al., 2017). The geological changes that occurred in this region are poorly understood, as is the chronostratigraphy, which is due to a lack of outcrop, haphazard, scant fossil remains and the widespread reworking of old sand and sediment (Wright et al., 2000). Geological maps of KwaZulu-Natal published by Geology Education Museum, University of KwaZulu-Natal (2020) suggests Cretaceous-aged deposits, and Walaszczyk et al. (2009) suggested that the Nibela Peninsula is upper Campanian in age.

Description—The left side of this partial vertebra is better preserved than the right as the left synapophysis is mostly complete. The left posterior zygopophysis (Figure 12A) and the left lamina of the neural arch (Figures 12A,F) are both present. Both prezygopophyses are absent as well as the neural spine and the poor preservation of the right side of the vertebra means that the neural arch is only preserved in part. As with all mosasauroids and most squamates, the vertebra is procoelous (Wiffen, 1990) (Figures 12C,D).

The condyle is smooth and almost complete. It is heart-shaped dorsally and rounded ventrally with straight lateral edges with a maximum width of 52.51 mm and a maximum height of 51.21 mm (Figure 12D). The center of the cotyle is smooth but the edges are poorly preserved with the dorsal portions as well as the right lateral and posterior edges of the cotyle face having been broken off (Figure 12C). Despite this, it seems reasonable to suggest that the cotyle was roughly circular in shape and has a maximum height of 52.72 mm and a total width of 44.96 mm; however, it is impossible to measure the exact width due to its incompleteness (Figure 12C). There is no evidence of zygosphenes due to poor preservation of the region anterior to the neural spine, but a left zygtrum is visible and has a triangular indentation medial to the posterior zygapophysis (Figure 12D), which implies that zygosphenes-zygantra complexes were present.

The left synapophysis is mostly complete with some evidence of surface wear (Figure 12F). The anterior surface of the transverse process is approximately in line with the center of the cotyle

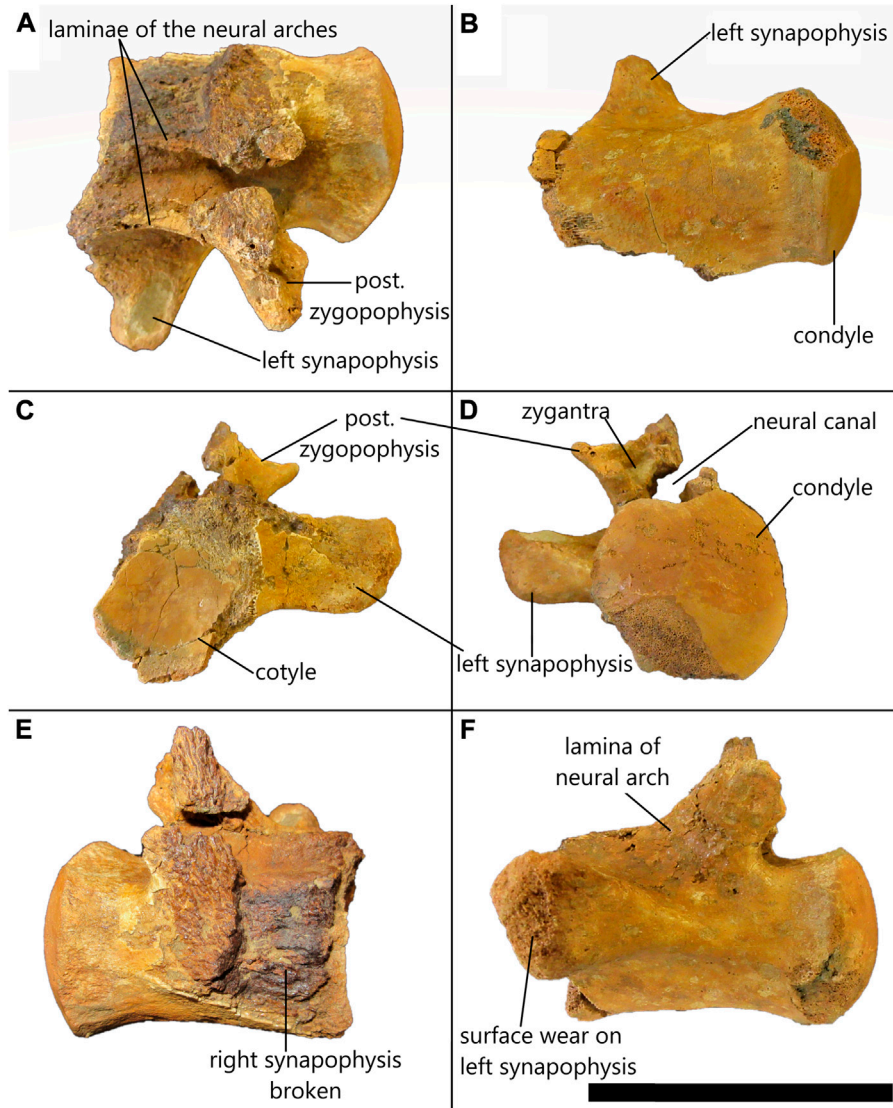


FIGURE 12
Indeterminate partial mosasaurid dorsal vertebra from St. Lucia in (A) dorsal, (B) ventral, (C) anterior, (D) posterior, (E) right lateral, (F) left lateral view. Scale bar = 80 mm.

(Figure 12C) and it originates about midway between the ventral and dorsal edges of the centrum (Figure 12F). It extends outwards and slightly dorsally (Figure 12D). The synapophysis is approximately 35.76 mm long measured from the base at the outer edge of the cotyle to the extremity, is approximately 25.80 mm high measured near the base and has an anteroposterior width of around 14.95 mm measured at the extremity. The extremity of the synapophysis is anteroposteriorly compressed and rounded at the edges (Figure 12F).

Due to the fragmentary nature of the right side of the vertebra, there is no evidence of the right posterior zygopophysis, nor is there direct evidence to suggest that the neural arches were fused. However, by the position of the medial

edge of the left neural arch above the neural canal (Figure 12D), it seems as though the neural arches were fused.

Discussion—The presence of synapophyses, which articulate with the ribs, as well as the relatively long length of the centrum (74.94 mm) suggests that this is a dorsal vertebra. In the posterior view (Figure 12D) the isolated vertebra from St Lucia looks like the sixteenth dorsal vertebra of *Plioplatecarpus primaevus*, which was described and figured by Holmes (1996, Figure 10C, p.682). The heart-shaped condyle (Figure 12D), the position and direction of extension of the synapophysis from the centrum, and the dorsoventral thickness of the

synapophysis (Figure 12C) indicate that it is one of the middle-to-last dorsal vertebrae before the first pygal vertebrae as with the *Pl. primaevus* sixteenth dorsal vertebra (Holmes, 1996).

The presence of a zygosphenes-zygantra complex (Figure 12D) in the isolated vertebra from St Lucia is problematic because this feature is absent in *Tylosaurus* and *Plioplatecarpus* (Russell, 1967; Jiménez-Huidobro et al., 2018). Therefore, despite similarities with *Pl. primaevus*, the presence of this diagnostic feature indicated that the St Lucia vertebra cannot belong to *Pl. primaevus*.

Zygosphenes and zygantra are features that are present and well-developed in *Clidastes*, *Prognathodon* (Lingham-Soliar and Nolf, 1990; personal observation at RBINS) and *Globidens* (Polcyn et al., 2010; Konishi and Caldwell, 2011) and present but not as well-developed in *Mosasaurus*, *Plotosaurus* and *Platecarpus* (except in cervical vertebrae) (Russell, 1967), among Mosasaurids. The dorsal vertebra of *M. hoffmannii* figured by Street and Caldwell, (2017, figure 18, p.545) shares some similarities with the vertebra from St Lucia although, the posterior zygapophyses are larger and extend far more laterally in the St Lucia vertebra than in *M. hoffmannii*. The zygantra at the base of the neural spine in the *M. hoffmannii* dorsal vertebra (Street and Caldwell, 2017) do not look like those triangular concavities suggested to be zygantra in the St Lucia vertebra. However, the difference in the shape of the zygosphenes and zygantra depends on the vertebral position. Russell (1967, figure 42, p.160) notes that the anterior vertebrae of *Plioplatecarpus primaevus* and *Platecarpus* are almost identical barring the absence of the zygosphenes-zygantra in *Plioplatecarpus*. There are similarities between the isolated vertebra from St Lucia and that of *Pl. primaevus* figured by Holmes (1996), however, due to the preservation and lack of other fossil evidence we assign the St Lucia vertebra to Plioplatecarpinae.

4 Age of the Pondoland Mosasaurids

Strontium isotope dating was performed on IT-1 (CGP/1/2265). Six readings produced the following means for $^{87}\text{Sr}/^{86}\text{Sr}$: 1) 0.707828 2) 0.707817 3) 0.707826 4) 0.707807 5) 0.707820 6) 0.707806. All readings yielded 2-sigma error values of 0.00030. The mean $^{87}\text{Sr}/^{86}\text{Sr}$ was calculated to be 0.707817 with a standard deviation of 0.000019. Using the look-up table Version 4 from McArthur et al. (2012) the numerical ages for each $^{87}\text{Sr}/^{86}\text{Sr}$ value could be calculated (see Supplementary Table S2). From the calibration curve adapted from McArthur et al. (2012) it appears that IT-1 from the CGP/1/2265 muzzle unit dates to the End Maastrichtian. The mean age was calculated to be 66.85 Ma (standard deviation = 0.46 Ma) approximately 850,000 years prior to the Cretaceous/Paleogene (K/Pg) extinction event that led to the extinction of the mosasaurids (amongst other organisms).

According to Rogers and Schwarz (1902), the Pondoland mosasaurid remains were found in a Santonian-aged deposit. However, in this study the use of strontium isotope dating has enabled more accurate dating of the CGP/1/2265 muzzle unit and isolated teeth: the results of the strontium isotope analysis of the enamel of IT-1 suggest that specimen CGP/1/2265 is Maastrichtian-aged with a mean $^{87}\text{Sr}/^{86}\text{Sr}$ of 0.707817, which equates to 66.84 Ma (using McArthur et al., 2012).

Unfortunately, dating CGP/1/2265 does not provide further information as to the relationship between it and the frontoparietal complex and dentary fragments (SAM-PK-5265). Strontium isotope analysis of enamel from one of the replacement teeth in the anterior dentary fragment (SAM-PK-5265) could resolve this issue and, if found to be Santonian-aged, would support its assignment to *Taniwhasaurus*. However, it was not possible to obtain permission for this due to the rarity of the specimen and the destructive nature of the strontium dating methods (thin sectioning + laser ablation/solution method). This information would also only provide clues to the relationship (or lack thereof) between the anterior dentary fragment and the CGP/1/2265 muzzle unit and isolated teeth, but it would not provide any further concrete information about the frontoparietal complex.

5 Concluding remarks and future research

There are characteristics of the SAM-PK-5265 frontoparietal complex that resemble *Taniwhasaurus*, along with the associated dentary fragments, as was suggested by Jiménez-Huidobro, (2016) and Jiménez-Huidobro and Caldwell (2019). However, two features that are present in all tylosaurine mosasaurs and are absent in SAM-PK-5265 (Jiménez-Huidobro and Caldwell, 2019) are: 1) external nares invading the frontal, and 2) internarial bar overlapping the anterior tip of the frontal. For that reason, the specimen cannot be assigned to either *Taniwhasaurus* or *Tylosaurus* origin, as was first put forward by Broom (1912) and supported by Jiménez-Huidobro et al. (2019). Moreover, these diagnostic features that exclude the frontoparietal complex from the tylosaurines support an assignment to cf. *Prognathodon*: 1) A lack of overlap of the frontal by the internarial bar and 2) an absence of narial embayment in the frontal is diagnostic for *Prognathodon* (Konishi et al., 2011). Other mosasaurine affinities include the anterior convergence of the anterior borders of the postorbitofrontal and a sinusoidal medial border of the postorbitofrontal in ventral view (Konishi et al., 2014). These features are both reminiscent of *M. missouriensis* (Konishi et al., 2014), further supporting its mosasaurine origin.

The anatomy and robustness of the elements present in the muzzle unit of CPG/1/2265 suggest affinities with the

TABLE 3 Summary of the SA mosasaurid material with information regarding the current specimen numbers for each element, the number of skeletal elements per individual, where the elements were recovered, the age of the elements and the suggested taxonomic assignment of each element based on this study. *This specimen will be housed at Iziko Museums of Cape Town, but it does not yet have a specimen number.

Specimen	Individual	Skeletal element	Locality	Age	Taxonomic assignment
SAM-PK-5265	A	Frontoparietal complex	Pondoland	End Maastrichtian	<i>Prognathodon</i>
SAM-PK-5265	A	Posterior dentary fragment	Pondoland	End Maastrichtian	<i>Prognathodon</i>
CGP/1/2265	A	Muzzle unit and isolated teeth	Pondoland	End Maastrichtian	<i>Prognathodon</i>
SAM-PK-5265	B	Anterior dentary fragment	Pondoland	Late Cretaceous (?Santonian)	<i>Taniwhasaurus</i>
*	C	Isolated vertebra	St Lucia	Late Cretaceous (?Campanian)	<i>Plioplatecarpinae</i>

genus *Prognathodon*; it is interpreted here as cf. *Prognathodon*. The isolated teeth from the muzzle unit closely resemble isolated teeth assigned to *P. currii* by Bardet et al. (2005). However, we find problems associated with the initial *P. currii* description (e.g., tooth surfaces not well-preserved in the type and only specimen, premaxillary suture margins unclear [see Christiansoen and Bonde, 2002]) that render the assignment of CGP/1/2256 to *P. currii* unreliable. The muzzle unit and associated isolated teeth (CGP/1/2265) are assigned to cf. *Prognathodon* (see Table 3, individual A).

Chinsamy-Turan et al. (2018), based on the matrix surrounding the fossils, and from the descriptions given by Rogers and Schwarz (1902) strongly suggested that the muzzle unit (CGP/1/2265) and the frontoparietal complex and dentary fragments (SAM-PK-5265) were found together in Pondoland, Eastern Cape. Chinsamy-Turan et al. (2018) considered the possibility that the specimens were, for unknown reasons, accessioned into different museum collections and that only the frontal/parietal unit of SAM-PK-5265 was described by Broom (1912). It seems that Broom (1912) interpreted the “lower jaw belonging to the reptilian genus Mosasaurus” as described in Rogers and Schwarz (1902, p. 41) as being the two dentary fragments associated with the frontoparietal complex (SAM-PK-5265). As proposed by Chinsamy-Turan et al. (2018), the alternative scenario is that the “lower jaw belonging to the reptilian genus Mosasaurus” was a reference to the unprepared muzzle unit, which at first glance, looks like a set of large mosasaur jaws. The dentary fragments are, by contrast, small, and unremarkable by comparison. The dimensions of the SAM-PK-5265 frontoparietal complex and the CGP/1/2265 muzzle unit correspond well to generate a picture of a large, heavy skull that is proportionally short, as is seen in other members of *Prognathodon*. The thickness of the frontal table is also congruent with it being a *Prognathodon*. In this case, it seems plausible that some of the elements of SAM-PK-5265 belong to the same individual as CGP/1/2265, though we make no such certain assignment here.

As described above, it seems, based on morphology, that the SAM-PK-5265 anterior dentary fragment belonged to the

same taxon as the frontoparietal complex and the posterior dentary fragment. The overall appearance of the anterior dentary fragment is that it is from a more gracile mosasaurid than *Prognathodon*. The replacement tooth visible in the anterior dentary fragment possesses smooth enamel with medial facets, which is not observed on the isolated teeth from the muzzle unit (CGP/1/2265). The replacement tooth in the anterior dentary fragment resembles the figured teeth of *Ta. mikasaensis*, from Japan (Caldwell et al., 2008). However, the replacement tooth in the anterior dentary fragment is straight, whereas *Ta. mikasaensis* has posteromedially recurved tooth crowns (Caldwell et al., 2008). The suggestion by Jiménez-Huidobro and Caldwell (2019) to assign it to *Taniwhasaurus* is accepted here, but it cannot be identified at the species level. We therefore interpret it here as cf. *Taniwhasaurus* (see Table 3, individual B).

Strontium isotope analysis of the CGP/1/2265 tooth dated this specimen to the Late Maastrichtian. Assuming that CGP/1/2265 and SAM-PK-5265 were indeed found together means that this entire collection of specimens are younger than the Santonian age that was originally proposed by Rogers and Schwarz (1902). *Prognathodon* specimens are known from the Early Campanian to End Maastrichtian deposits around the world (Russell, 1967; Konishi et al., 2011). Up-to-date and detailed research on the stratigraphy of these areas would make it easier to assign fossils more accurately to specific ages. The development of less destructive dating methods in the future could allow for the age of the SAM-PK-5265 anterior dentary fragment to be determined, which would provide more concrete evidence of its taxonomy and relation (or lack thereof) to the other specimens.

The anatomical assessment of the isolated partial vertebra from St Lucia shows that it closely resembles one of the middle-to-last dorsal vertebrae of *Pl. primaevus* figured by Holmes (1996), but it possesses a zygosphenes-zygantra complex, which could indicate affinities with *Platecarpus*. It is herein assigned to cf. *Plioplatecarpinae* (Table 3).

More intensive fieldwork and fossil exploration all along the east coast of SA would surely yield more specimens and possibly

even new taxa. This would add to the countries' already rich fossil heritage and could aid in the understanding of the diversity, origins, and dispersal of mosasaurs in and around Southern Africa.

Data availability statement

The original contributions presented in the study are included in the article/Supplementary Material, further inquiries can be directed to the corresponding author.

Author contributions

The paper is derived from MRW Masters thesis (completed in 2020) for which AC supervised and MWC co-supervised. The bulk of the research and writing was thus done by MRW and assisted by AC and MWC.

Acknowledgments

We thank, R. Redelstorff, South African Heritage Resources Agency; K. Nzolo and N. Mchunu, Geosciences Council, for access to CGP/1/2265; Z. Skosan and C Browning, Iziko South African Museums, Cape Town for access to SAM-PK-5265; S. Riddles, Iziko Museums, Cape Town for their careful preparation of CGP/1/2265, and P. Le Roux, Department of Geological Sciences, University of Cape Town (UCT), for guidance with strontium isotope analysis. MRW thanks A. Folie and colleagues at the Royal Belgium Institute of Natural Sciences for access to mosasaur collections. The National Research Foundation (NRF), African Origins Platform grant (number 117716) to AC is acknowledged for having provided a grant holder linked

References

- Bardet, N., Suberbiola, X. P., Iarochene, M., Amalik, M., and Bouya, B. (2005). Durophagous mosasauridae (squamata) from the upper cretaceous phosphates of Morocco, with description of a new species of *Globidens*. *Geol. Mijnb.* 83 (3), 167–175. doi:10.1017/S0016774600020953
- Broom, R. (1912). *On a species of Tylosaurus from the upper cretaceous beds of Pondoland*.
- Bullard, T. S., and Caldwell, M. W. (2010). Redescription and rediagnosis of the tylosaurine mosasaur *Hainosaurus pembinensis* Nicholls, 1988, as *Tylosaurus pembinensis* (Nicholls, 1988). *J. Vertebrate Paleontology* 30 (2), 416–426. doi:10.1080/02724631003621870
- Caldwell, M. W., Holmes, R., Bell, G. L., and Wiffen, J. (2005). An unusual tylosaurine mosasaur from New Zealand: A new skull of *Taniwhasaurus oweni* (lower haumurian; upper cretaceous). *J. Vertebrate Paleontology* 25 (2), 393–401. doi:10.1671/0272-4634(2005)025[0393:autmf]2.0.co;2
- Caldwell, M. W., Konishi, T., Obata, I., and Muramoto, K. (2008). A new species of *Taniwhasaurus* (mosasauridae, Tylosaurinae) from the upper santonian-lower campanian (upper cretaceous) of Hokkaido, Japan. *J. Vertebr. Paleontol.* 28 (2), 339–348. doi:10.1671/0272-4634(2008)28[339:ansotm]2.0.co;2
- Caldwell, M. W. (2007). *Ontogeny, anatomy and attachment of the dentition in mosasaurs*. Mosasauridae: Squamata, 687
- Chin, K., Bloch, J., Sweet, A., Tweet, J., Eberle, J., Cumbaa, S., et al. (2008). Life in a temperate polar sea: A unique taphonomic window on the structure of a late cretaceous arctic marine ecosystem. *Proc. R. Soc. B*, 275, 2675–2685. doi:10.1098/rspb.2008.0801
- Chinsamy, A., and Raath, M. A. (1992). Preparation of fossil bone for histological examination. *Palaeontol. Afr.* 29 (3).
- Chinsamy, A., Tunogllf, C., and Thomas, D. B. (2012). Dental microstructure and geochemistry of *Mosasaurus hoffmannii* (squamata: Mosasauridae) from the late cretaceous of Turkey. *Bull. Soc. Geol. Fr.* 183 (2), 85–92. doi:10.2113/gssgfbull.183.2.85
- Chinsamy-Turan, A., Klinger, H., Shelton, C., Montoya-Sanhueza, G., Krupandan, E., Maharaj, I., et al. (2018). *Rare dinosaur, mosasaur, turtle, and other vertebrate remains from marine Cretaceous deposits of South Africa*. Paris: 5th International Paleontological Congress. [poster].
- Christiansen, P., and Bonde, N. (2002). A new species of gigantic mosasaur from the late cretaceous of Israel. *J. Vertebrate Paleontology* 22 (3), 629–644. doi:10.1671/0272-4634(2002)022[0629:ansogm]2.0.co;2

bursary and funding support for collections visit to Brussels for MRW, as well as for funding the field trip to St Lucia that led to the finding of the mosasaur vertebra. H. Klinger, C. Shelton, E. Krupandan, G. Montoya-Sanhueza, I. Maharaj, and AC comprised the St. Lucia fieldtrip team, and are thanked for their efforts. Opinions expressed and conclusions arrived at, are those of the authors and are not necessarily attributed to the NRF. MRW thanks AC: the UCT Palaeobiology Lab Group for guidance and support during this research project. We thank two reviewers whose comments significantly improved this paper.

Conflict of interest

The authors declare that the research was conducted in the absence of any commercial or financial relationships that could be construed as a potential conflict of interest.

Publisher's Note

All claims expressed in this article are solely those of the authors and do not necessarily represent those of their affiliated organizations, or those of the publisher, the editors and the reviewers. Any product that may be evaluated in this article, or claim that may be made by its manufacturer, is not guaranteed or endorsed by the publisher.

Supplementary Material

The Supplementary Material for this article can be found online at: <https://www.frontiersin.org/articles/10.3389/feart.2022.971968/full#supplementary-material>

- Compagno, L. J. V. (1990). Relationships of the megamouth shark, *Megachasma pelagios* (Lamniformes: Megachasmidae), with comments on its feeding habits. *Systematics* 5, 1
- Copeland, S. R., Sponheimer, M., le Roux, P. J., Grimes, V., Lee-Thorp, J. A., de Ruiter, D. J., et al. (2008). Strontium isotope ratios ($^{87}\text{Sr}/^{86}\text{Sr}$) of tooth enamel: A comparison of solution and laser ablation multicollector inductively coupled plasma mass spectrometry methods. *Rapid Commun. Mass Spectrom.* 22, 3187–3194. doi:10.1002/rcm.3717
- Dortangs, R. W., Schulp, A. S., Mulder, E. W., Jagt, J. W., Peeters, H. H., and de Graaf, D. T. (2002). A large new mosasaur from the Upper Cretaceous of The Netherlands. *Neth. J. Geosciences* 81 (1), 1–8. doi:10.1017/S0016774600020515
- Ellis, R. (2003). *Sea dragons: Predators of the prehistoric oceans*. Lawrence Kansas: University Press of Kansas.
- Fernandez, M., and Martin, J. E. (2009). Description and phylogenetic relationships of *Taniwhasaurus antarcticus* (mosasauridae, Tylosaurinae) from the upper campanian (cretaceous) of Antarctica. *Cretac. Res.* 30 (3), 717–726. doi:10.1016/j.cretres.2008.12.012
- Gomes, M., et al. (2017). “Diatom-inferred hydrological changes and Holocene geomorphic transitioning of Africa’s largest estuarine system, Lake St Lucia”, Estuarine,” in *Coastal and shelf science* (Elsevier), 170–180. doi:10.1016/j.ecss.2017.03.030
- Grigoriev, D. V. (2013). Redescription of *Prognathodon lutugini* (squamata, mosasauridae) ?реописание. *Prognathodon Lutugini (Squamata, Mosasauridae)* 317113 (3), 246
- Holmes, R. (1996). *Plioplatecarpus primaevus* (mosasauridae) from the Bearpaw Formation (campanian, upper cretaceous) of the north American western interior seaway. *J. Vertebr. Paleontol.* 16 (4), 673–687. doi:10.1080/02724634.1996.10011357
- Jiménez-Huidobro, P. A. (2016). *Phylogenetic and palaeobiogeographical analysis of Tylosaurinae (squamata: Mosasauridae)*. Unpublished doctoral dissertation. Alberta, Canada: University of Alberta.
- Jiménez-Huidobro, P., and Caldwell, M. W. (2019). A new hypothesis of the phylogenetic relationships of the Tylosaurinae (Squamata: Mosasauridae). *Front. Earth Sci. (Lausanne)*, 7, 1–15. doi:10.3389/feart.2019.00047
- Jiménez-Huidobro, P., and Caldwell, M. W. (2016) ‘Reassessment and reassignment of the early mastrichtian mosasaur *Hainosaurus bernardi* Dollo, 1885, to *Tylosaurus* marsh, 1872, 36, 1096257. doi:10.1080/02724634.2016.1096275
- Jiménez-Huidobro, P., et al. (2018). A new species of tylosaurine mosasaur from the upper Campanian Bearpaw Formation of Saskatchewan, Canada. *J. Sys. Palaeontol.* Alberta: Taylor & Francis. doi:10.1080/14772019.2018.1471744
- Konishi, T., Brinkman, D., Massare, J. A., and Caldwell, M. W. (2011). New exceptional specimens of *Prognathodon overtoni* (squamata, mosasauridae) from the upper campanian of Alberta, Canada, and the systematics and ecology of the genus. *J. Vertebrate Paleontology* 31 (5), 1026–1046. doi:10.1080/02724634.2011.601714
- Konishi, T., and Caldwell, M. W. (2011). Two new plioplatecarpine (Squamata, Mosasauridae) genera from the Upper Cretaceous of North America, and a global phylogenetic analysis of plioplatecarpines. *J. Vertebrate Paleontology* 31 (4), 754–783. doi:10.1080/02724634.2011.579023
- Konishi, T., Newbrey, M. G., and Caldwell, M. W. (2014). A small, exquisitely preserved specimen of *Mosasaurus missouriensis* (Squamata, Mosasauridae) from the upper Campanian of the Bearpaw Formation, Western Canada, and the first stomach contents for the genus. *J. Vertebrate Paleontology* 34 (4), 802–819. doi:10.1080/02724634.2014.838573
- Le Roux, P. J. (2010). Lithium isotope analysis of natural and synthetic glass by laser ablation MC-ICP-MS. *J. Anal. At. Spectrom.* 25 (7), 1033–1038. doi:10.1039/b920341a
- Lingham-Soliar, T., and Nolf, D. (1990). *The mosasaur Prognathodon (reptilia, mosasauridae) from the upper cretaceous of Belgium*. Brussels: Bulletin of the Royal Belgian Institute of Natural Sciences.
- Lingham-Soliar, T. (1992). *The tylosaurine mosasaurs (reptilia, mosasauridae) from the upper cretaceous of Europe and Africa*, 62. Brussels: Bulletin of the Royal Belgian Institute of Natural Sciences, 171.
- Liu, K. W., and Greyling, E. H. (1996). Grain-size distribution and cementation of the cretaceous Mzamba Formation of eastern Cape, south Africa: A case study of a storm-influenced offshore sequence. *Sediment. Geol.* 107 (1–2), 83–97. doi:10.1016/s0037-0738(96)00020-6
- Martin, J. E., and Fernandez, M. (2007). The synonymy of the late cretaceous mosasaur (squamata) genus *lakumasaurus* from Antarctica with *Taniwhasaurus* from New Zealand and its bearing upon faunal similarity within the weddellian province. *Geol. J.* 42, 203–211. doi:10.1002/gj.1066
- McArthur, J. M., Howarth, R. J., and Shields, G. A. (2012). Strontium isotope stratigraphy. *Geol. Time Scale* 1–2, 127–144. doi:10.1016/B978-0-444-59425-9.00007-X
- Polcyn, M. J., Jacobs, L. L., Schulp, A. S., and Mateus, O. (2010). The north african mosasaur *Globidens phosphaticus* from the mastrichtian of Angola. *Hist. Biol.* 22 (1), 175–185. doi:10.1080/08912961003754978
- Ramos, F. C., Wolff, J. A., and Tollstrup, D. L. (2004). Measuring $^{87}\text{Sr}/^{86}\text{Sr}$ variations in minerals and groundmass from basalts using LA-MC-ICPMS. *Chem. Geol.* 211 (1–2), 135–158. doi:10.1016/j.chemgeo.2004.06.025
- Rogers, A. W., and Schwarz, E. H. L. (1902). *Annual report of the geological commission 1900*. Cape Town: Department of Agriculture.
- Russell, D. a. (1967). *Systematics and morphology of American mosasaurs*. New Haven, Connecticut: Bulletin 23 of the Peabody Museum of Natural History Yale University.
- Shimada, K., and Cicimurri, D. J. (2005). Skeletal anatomy of the late cretaceous shark, *Squalicorax* (Neoselachii: Anacoracidae). *Palaontol. Z.* 79 (2), 241–261. doi:10.1007/bf02990187
- Stewart, R. F., and Mallon, J. (2018). Allometric growth in the skull of *Tylosaurus* proriger (Squamata: Mosasauridae) and its taxonomic implications. *Vert. Anat. Morph. Palaeo.* 6, 75–90. doi:10.18435/vamp29339
- Street, H. P., and Caldwell, M. W. (2017). Rediagnosis and redescription of *Mosasaurus hoffmannii* (Squamata: Mosasauridae) and an assessment of species assigned to the genus *Mosasaurus*. *Geol. Mag.* 154, 521–557. doi:10.1017/S0016756816000236
- Susela, Z. (2014). *Stratigraphy and sedimentology of the Mzamba Formation in the eastern Cape, South Africa*. Doctoral dissertation, University of Fort Hare.
- University of KwaZulu-Natal (2020). KwaZulu-natal geological map and cross sections’, geology education museum. Available at: www.stec.ukzn.ac.za/GeologyEducationMuseum/KZNGeology/KZNGeologyMap.aspx.
- Walaszczyk, I., Kennedy, W. J., and Klinger, H. C. (2009). Cretaceous faunas from zuluand and natal, south Africa. Systematic palaeontology and stratigraphical potential of the upper campanian-maastichtian inoceramidae (Bivalvia). *Afr. Nat. Hist.* 5 (1), 49.
- Wiffen, J. (1980). *Moanasaurus, a new genus of marine reptile (family mosasauridae) from the upper cretaceous of north Island*. New Zealand’, 8306. doi:10.1080/00288306.1980.10424122
- Wiffen, J. (1990). New mosasaurs (reptilia; family mosasauridae) from the upper cretaceous of North Island, New Zealand. *N. Z. J. Geol. Geophys.* 33 (1), 67–85. doi:10.1080/00288306.1990.10427574
- Wright, C. I., Miller, W. R., and Cooper, J. A. G. (2000). The late cenozoic evolution of coastal water bodies in northern kwazulu-natal, south Africa. *Mar. Geol.* 167 (3–4), 207–229. doi:10.1016/S0025-3227(00)00032-3